Regio- and Size-Selective Catalysis:
Porous Aromatic Frameworks and C3-Symmetric Receptors

by

Anont Tanaset

B.A., Chemistry, 2014
Columbia University

Submitted to the Department of Chemistry
in Partial Fulfillment of the Requirements for the Degree of

MASTER OF SCIENCE
IN CHEMISTRY

at the

Massachusetts Institute of Technology

September 2016

Signature of Author: Signature redacted
Department of Chemistry
August 18, 2016

Certified by: Signature redacted
Jeffrey F. Van Humbeck
Thesis Supervisor

Accepted by: Signature redacted
Robert W. Field
Chairman, Departmental Committee on Graduate Students

Regio- and Size-Selective Catalysis:
Porous Aromatic Frameworks and C3-Symmetric Receptors

by

Anont Tanaset

Submitted to the Department of Chemistry
on August 18, 2016 in Partial Fulfilment of the
Requirements for the Degree of Master of Science
in Organic Chemistry

ABSTRACT

Porous aromatic frameworks (PAFs) have recently emerged as a new class of materials with impressive stability and high surface area, which led to their applications in gas storage and small molecule recognition. Herein, the synthesis and functionalization of PAFs were described, and their potential use as selective oligomerization for fuel upgrading was investigated. However, functionalized PAFs showed undesired reactivity possibly due to low rate of substrate and product diffusion in and out of the framework. On the other hand, a novel C3-symmetric hydrogen bonding receptor was synthesized and investigated for its use as size- and regioselective catalyst. It was demonstrated that the receptor was able to distinguish substrates with different functional groups in binding experiments, and was able to improve S_N2 reaction yield although with some significant limitations.

Thesis Supervisor: Jeffrey F. Van Humbeck
Title: Assistant Professor of Chemistry

Anont Tanaset graduated from Columbia University with departmental honors in 2014 with a Bachelor of Arts in Chemistry after working in the research lab of Tristan Lambert. During his time at Columbia, he contributed to a publication in Chemistry – A European Journal: *'Phase-Transfer and Other Types of Catalysis with Cyclopropenium Ions.'* He then joined the research lab of Jeffrey Van Humbeck at the Massachusetts Institute of Technology for his graduate studies, where he explored the uses of porous aromatic frameworks (PAFs), organic cages, and C3-symmetric receptors as size- and regioselective catalysts. In summer 2016, he also received the Kenneth M. Gordon Scholarship.

Table of Contents

1.0 Introduction

1.1 Size- and Shape-Selective Catalysis

The design and synthesis of catalysts for specific purposes has always been an ongoing challenge for both academia and industry. While many synthetic catalysts are now designed as general catalysts that can be used with a broad range of substrates, substrate-selective catalysis, whether by size or shape of the substrates, remains important and is crucial for many industrial processes especially where the reaction of interest is performed with a substrate pool that cannot be easily separated or purified.[1]

Heterogeneous substrate-selective catalysts are dominated by zeolites and other porous materials while most homogeneous substrate-selective catalysts are biologically-inspired.[1]

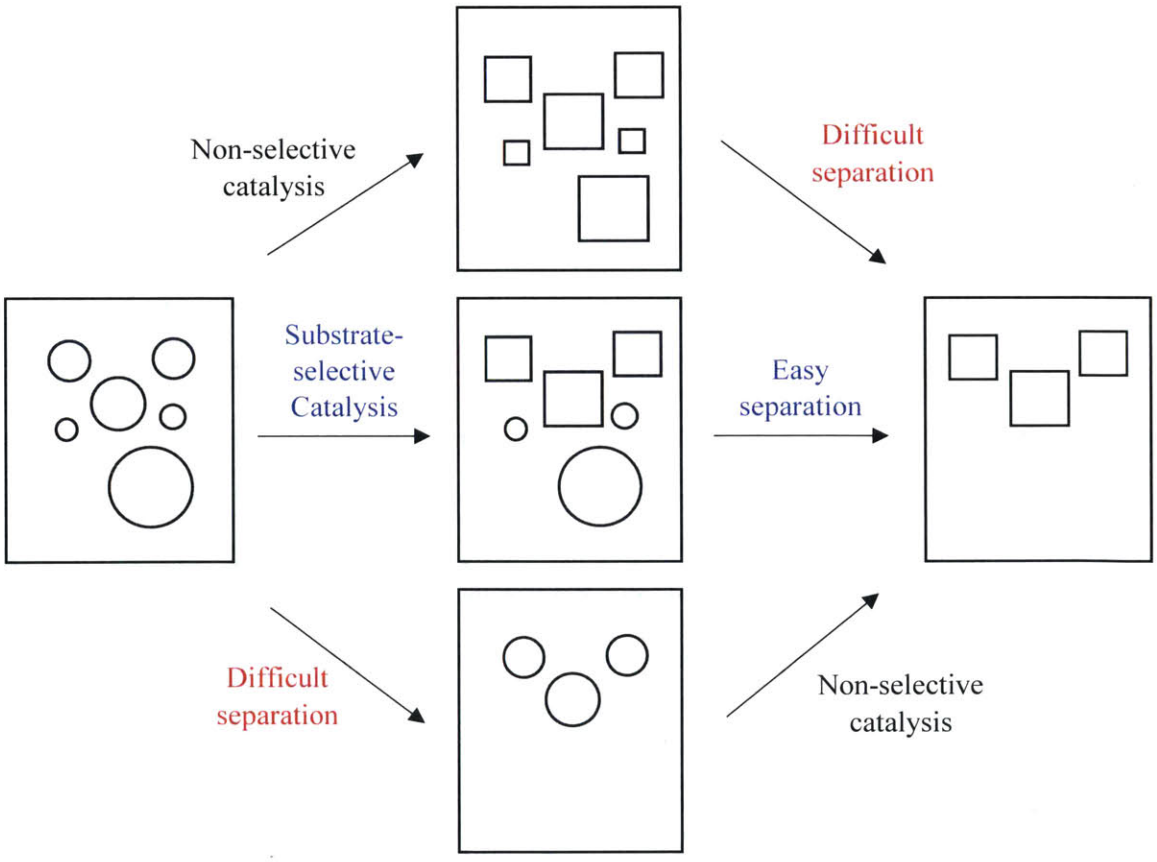

Figure 1. Example of useful case for substrate-selective catalysis.

However, in order to achieve desired selectivity in either system, many considerations have to be taken into account from selecting appropriate binding group to controlling the exact size and shape of the pore space of the system, most of which are still a challenge. Common existing platforms for substrate-selective catalysis include metalloporphyrin complexes, especially for selective epoxidation of alkenes. In 1990, Collman et al reported the synthesis of manganese "picnic basket porphyrins", which show shape-selectivity for alkene epoxidation as high as >1000:1 in the case of *cis*-2-octene versus *cis*-cyclooctene and more than 70:1 in several other cases.[2,3] The system has a cavity that restricts large alkenes from approaching the active site.

Although many other biologically-inspired systems have been developed, substrate-selective catalysis in industry is still limited to just a few catalysis platforms, specifically the use of zeolites.[1] Zeolite catalysts are used in industry for many applications such as the steam cracking of hydrocarbons to short-chain alkenes. In the process of shape-selective steam cracking, the crystalline space of the zeolite catalyst keeps the branched hydrocarbons from getting to the catalytic site, producing exclusively the linear fragment products. This process of steam cracking and properties of zeolite were explored and reported in details by Weisz during 1960-1980.[4] Detailed reviews of zeolite and zeolite catalysis can be found in the references.[5–7]

Seeing that substrate-selective catalysis is still relatively underexplored and underused especially on industrial scale, we aimed to develop new platforms for size- and shape-selective catalysis by exploring the potential of recently discovered materials and molecules, namely, porous aromatic frameworks and C3-symmetric receptors.

1.2 Porous Aromatic Frameworks

Porous aromatic frameworks, or PAFs, are a group of microporous organic polymers well known for their high surface areas and physicochemical stability. The term PAF was first used by

Ben et al. in 2009 in their reported synthesis of PAF-1, which has Brunauer–Emmett–Teller (BET) surface area of 5640 m^2g^{-1} and Langmuir surface area of 7100 m^2g^{-1}, a world record among similar type of materials at the time of their first discovery.[8] PAF-1 and related materials also have very high uptake of carbon dioxide and hydrogen, which created interest among researchers as potential candidates for gas storage applications.[9,10]

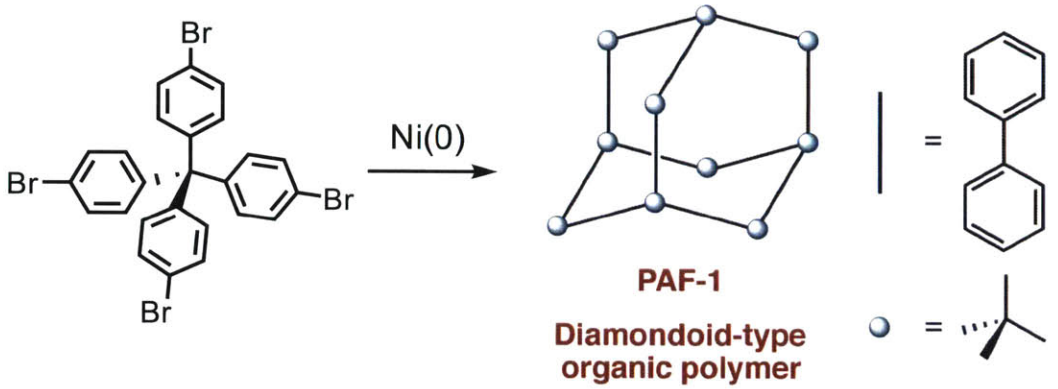

Figure 2. Structure of PAF-1.

The origin of the high surface area and physicochemical stability comes from the similarity between PAF-1 structure and that of diamond.[11] By replacing each C–C bond of diamond's tetrahedral framework with 4,4'-biphenyl linkers, the strong tetrahedral structure remains the same while creating more internal surface area from the surface of phenyl rings. From this rigid structure, most PAFs have been reported to be insoluble in organic solvents, and can retain their integrity in boiling water or cold acid or base bath. The high surface area of PAFs can also be attribute to the lack of halogen ending groups, which can be achieved via irreversible Yamamoto-type Ullmann cross-coupling reaction. It is worth noting that from powder X-ray diffraction (PXRD), PAF-1 is mostly amorphous, which means that the high surface area of PAFs does not arise from having highly ordered porous network, but rather from the combination of having rigid biphenyl framework, *dia* topology, and the lack of halogen end group.[10,11]

Due to the impressive gas absorption capability and stability of PAFs compared to other porous materials such as zeolites, metal organic frameworks (MOFs), and porous silicas, multiple applications of PAFs have been reported in the area of gas storage and small molecule recognition in recent years.[10,12–16] In many reports, PAFs show excellent stability over multiple absorption cycles and can be modified to possess high selectivity for the desired gas. Although the applications of PAFs for gas storage are beyond the scope of this thesis, many useful functionalization of PAFs resulted from these reports are used in our work. A work of particular interest is the amine introduction method developed by the Zhou group in 2012 in which polyamine groups are attached to PAF-1 framework via PAF-1-CH_2Cl. The presence of CO_2-philic amine groups was reported to increase CO_2 uptake from 1.3 mmol·g^{-1} (5.4 wt %) (PAF-1) to 4.3 mmol·g^{-1} (15.8 wt %) (PAF-1-CH_2DETA) at 295 K and 1 bar.[14]

The versatility of PAFs, together with the high surface areas and physicochemical stability, makes them a great candidate for heterogeneous catalysts. The Corma Group and Ma Group reported in 2013 and 2014 respectively a dual functionalization of PAF-1 with both acid and base on the biphenyl linker.[17,18] The functionalized PAF-1-$NHCH_2CH_2NH_2$-SO_3H was used as a heterogeneous cascade catalyst for deacetalization-Henry reaction, which proceeds successfully when both strong acid and strong base groups are present. The Ma group also reported the use of the same functionalized PAF-1 for Knoevenagel reaction of two substrates with different sizes and shapes (benzaldehyde and benzophenone). The catalyst was found to catalyze benzaldehyde in high yield while a low yield (8%) was observed for benzophenone. Even though the difference in reactivity might not have been caused solely from the size/shape difference of the substrates since these two substrates possess different innate reactivity, this report shows the potential of PAFs as size- and shaped-selective catalysts, which is the basis of our work in this thesis.

1.3 Selective-Oligomerization of Ethanol for Fuel-Upgrading

Ethanol has been recognized among chemists as a promising renewable energy source as it can be obtained from biomass. However, ethanol is not as efficient as butanol or hexanol in terms of its efficiency as a fuel due to its lower energy density and incompatibility with unmodified engines.[19] Therefore, an efficient process that can directly convert ethanol to butanol or hexanol is desirable. One of the reactions that has this capability is the Guerbet reaction, which uses borrowed hydrogen chemistry.[20] The short-chain alcohol starting materials first undergo dehydrogenation into an aldehyde, couples via aldol reaction with another aldehyde molecule, then undergoes dehydration and hydrogenation to give long-chain alcohol products.[19,21]

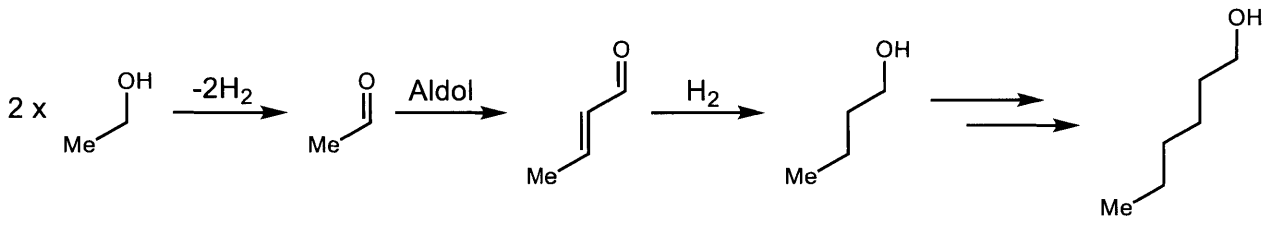

Scheme 1. Reaction scheme of Guerbet reaction.

However, even after numerous efforts and the discovery of new catalysts, the Guerbet reaction still offers less-than-ideal yields and selectivity, usually producing mixture of short- and long-chain, linear and branched oligomeric products. Our goal in this thesis was then to develop a system based on functionalized porous aromatic frameworks that would selectively catalyze aldol reactions within the pore space, using the pore size as the size-selective component. Starting materials and products would be allowed to enter and leave the catalytic site freely to prevent product inhibition, but the size of the pore will prevent undesired transition states.

1.4 C3-Symmetic Receptors

Over the past few years there have been a number of reports on synthetic receptors for selective recognition of small molecules and ions. Among these receptors, many of them have three binding arms pointing toward the same direction, forming a C3-symmetric binding "pocket" that can be adjusted in terms of size, shape, and binding functional groups.[22] The versatility of this scaffold has led to the development of C3-symmetric receptors for numerous purposes such as selective recognition of carbohydrates, selective recognition of cations and anions of different sizes, fullerene receptors, and many more.[23–27]

One promising precursor to several receptors is 1,3,5-tris(bromomethyl)-2,4,6-triethylbenzene **1**, which is a hexasubstituted benzene ring first reported by Walsdorff et al. in 1996.[28] Structure **1** exhibits an important characteristic by having the three ethyl groups at 1, 3, and 5 positions pointing to the same face of the molecule, while the bromomethyl groups are all pointing to the opposite face, creating a fully alternating up-down *ababab* conformation. Synthetic "arms" with desired functional groups can then be connected to each of the three bromomethyl groups, forming C3-symmetric receptors of choice. We envision that this precursor has potential as the main scaffold in our novel catalyst designs. In this thesis, we will explore the capability of C3-symmetric receptor's binding pocket as catalytic binding site via careful functional groups positioning and modifications.

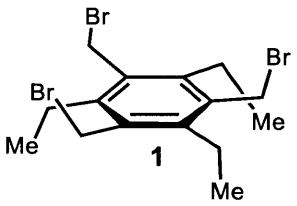

Figure 3. Structure of C3-symmetric receptor precursor **1**.

1.5 Hydrogen Bond Catalysis

Hydrogen bonding plays crucial roles in nature from protein folding, DNA bases pairing, to binding between substrate and enzyme.[29] It has also been known to catalyze a wide range of chemical processes by activating an electrophile or hydrogen-bond acceptor toward nucleophilic

attack.[30] In recent years, many small-molecule hydrogen-bonding catalysts have been synthesized with several different catalytic modes, either via single or double hydrogen bonding for electrophile activation.[31] However, simultaneous donation of multiple hydrogen bonds such as those in Jacobsen's thiourea catalyst systems has been found to be particularly effective compared to single hydrogen bond donation, possibly due to the higher level of preorganization and increased stabilization, which become especially useful in the field of asymmetric catalysis.[32]

The strength of a hydrogen bond can vary from 0.4 to 40 kcal mol^{-1} depending on the nature of both hydrogen-bond donor and acceptor, and the bond angle range appropriate for hydrogen bonding is quite broad from 90 to 180 degree, especially when the main interaction is electrostatic.[29,33] This characteristic, together with the relative ease of incorporating hydrogen-bond donor groups into organic molecules, makes hydrogen-bonding a useful interaction for our substrate-selective catalyst design, specifically for the C3-symmetric receptor catalysts. We envisioned that receptors with three hydrogen-bond donor groups facing toward the same face would create a binding pocket with unique properties that can act as substrate-selective catalytic binding site. The sensitivity of the strength of hydrogen bonding to bond angle and distance would also help the catalyst to bind preferentially to a specific substrate site when multiple binding sites are possible, which would create the potential of using our catalyst for positional selective or regioselective reaction.

1.6 Scope of Thesis Work

In this thesis, we aim to explore porous aromatic frameworks and C3-symmetric receptors as potential size- and shape- selective catalytic systems. The second chapter focuses on the development of functionalized porous aromatic frameworks, their physicochemical properties, and their catalytic activities in aldol reaction. The third chapter gives the details on development on

synthesis of C3-symmetric receptors, the binding studies of these receptors, and their potential as regioselective hydrogen-bonding catalysts. The fourth and fifth chapters provide discussion and conclusion for the thesis. Finally, the sixth chapter includes supporting information and procedure for all relevant syntheses.

References

(1) Lindbäck, E.; Dawaigher, S.; Wärnmark, K. *Chem. - A Eur. J.* **2014**, *20* (42), 13432–13481.
(2) Collman, J. P.; Zhang, X.; Hembre, R. T.; Braumanla, J. I. *J. Am. Chem. Soc.* **1990**, *112* (19), 5356–5357.
(3) Collman, J.; Zhang, X.; Lee, V.; Uffelman, E.; Brauman, J. *Science (80-.).* **1993**, *261* (5127), 1404–1411.
(4) Weisz, P. B. In *Studies in Surface Science and Catalysis*; 1981; Vol. 7, pp 3–20.
(5) Jacobs, P. A.; Flanigen, E. M.; Jansen, J. C.; van Bekkum, H. *Introduction to Zeolite Science and Practice*; Studies in Surface Science and Catalysis; Elsevier Science, 2001.
(6) Van Steen, E.; Callanan, L. H.; Claeys, C. *Recent Advances in the Science and Technology of Zeolites and Related Materials: Proceedings of the 14th International Zeolite Conference, Cape Town, South Africa, 25-30th April 2004*; Elsevier, 2004.
(7) Xu, R.; Chen, J.; Gao, Z.; Yan, W. *From Zeolites to Porous MOF Materials - the 40th Anniversary of International Zeolite Conference, 2 Vol Set: Proceedings of the 15th International Zeolite Conference, Beijing, P. R. China, 12-17th August 2007*; Studies in Surface Science and Catalysis; Elsevier Science, 2007.
(8) Ben, T.; Ren, H.; Ma, S.; Cao, D.; Lan, J.; Jing, X.; Wang, W.; Xu, J.; Deng, F.; Simmons, J. M.; Qiu, S.; Zhu, G. *Angew. Chemie - Int. Ed.* **2009**, *48* (50), 9621–9624.
(9) Pei, C.; Ben, T.; Qiu, S. *Mater. Horiz.* **2015**, *2* (1), 11–21.
(10) Lu, A.-H.; Hao, G.-P. *Annu. Reports Sect. "A" (Inorganic Chem.* **2013**, *109*, 484.
(11) Ben, T.; Qiu, S. *CrystEngComm* **2013**, *15* (1), 17–26.
(12) Van Humbeck, J. F.; McDonald, T. M.; Jing, X.; Wiers, B. M.; Zhu, G.; Long, J. R. *J. Am. Chem. Soc.* **2014**, *136* (6), 2432–2440.
(13) Lu, W.; Yuan, D.; Zhao, D.; Schilling, C. I.; Plietzsch, O.; Muller, T.; Bräse, S.; Guenther, J.; Blümel, J.; Krishna, R.; Li, Z.; Zhou, H.-C. *Chem. Mater.* **2010**, *22* (21), 5964–5972.
(14) Lu, W.; Sculley, J. P.; Yuan, D.; Krishna, R.; Wei, Z.; Zhou, H.-C. *Angew. Chemie - Int. Ed.* **2012**, *124* (30), 7480–7484.
(15) Yuan, D.; Lu, W.; Zhao, D.; Zhou, H.-C. *Adv. Mater.* **2011**, *23* (32), 3723–3725.
(16) Kizzie, A. C.; Dailly, A.; Perry, L.; Lail, M. A.; Lu, W.; Nelson, T. O.; Cai, M.; Zhou, H. *Mater. Sci. Appl.* **2014**, *05* (06), 387–394.
(17) Merino, E.; Verde-Sesto, E.; Maya, E. M.; Iglesias, M.; Sánchez, F.; Corma, A. *Chem. Mater.* **2013**, *25* (6), 981–988.
(18) Zhang, Y.; Li, B.; Ma, S. *Chem. Commun.* **2014**, 1–6.
(19) Sun, J.; Wang, Y. *ACS Catal.* **2014**, *4* (4), 1078–1090.
(20) Guerbet, M. *C.R. Acad. Sci. Paris* **1899**, *128*, 511.
(21) Kozlowski, J. T.; Davis, R. J. *ACS Catal.* **2013**, *3* (7), 1588–1600.

(22) Simaan, S.; Siegel, J. S.; Biali, S. E. *J. Org. Chem.* **2003**, *68* (9), 3699–3701.
(23) Cacciarini, M.; Cordiano, E.; Nativi, C.; Roelens, S. *J. Org. Chem.* **2007**, *72* (10), 3933–3936.
(24) Sather, A. C.; Berryman, O. B.; Moore, C. E.; Rebek, J. *Chem. Commun.* **2013**, *49* (57), 6379–6381.
(25) Chin, J.; Walsdorff, C.; Stranix, B.; Oh, J.; Chung, H. J.; Park, S. M.; Kim, K. *Angew. Chemie - Int. Ed.* **1999**, *38* (18), 2756–2759.
(26) Arda, A.; Venturi, C.; Nativi, C.; Francesconi, O.; Gabrielli, G.; Canada, F. J.; Jimenez-Barbero, J.; Roelens, S. *Chem. - A Eur. J.* **2010**, *16* (2), 414–418.
(27) Fukawa, M.; Sato, T.; Kabe, Y. *Chem. Commun.* **2015**, *51* (79), 14746–14749.
(28) Walsdorff, Christian; Saak, Wolfgang; Pohl, S. *J. Chem. Res. Synopses* **1996**, No. 6, 282–283.
(29) Desiraju, G. R.; Steiner, T. *The Weak Hydrogen Bond in Structural Chemistry and Biology*; Oxford University Press: Oxford, 1999.
(30) Schreiner, P. R. *Chem. Soc. Rev.* **2003**, *32* (5), 289–296.
(31) Pihko, P. M. *Angew. Chemie - Int. Ed.* **2004**, *43* (16), 2062–2064.
(32) Taylor, M. S.; Jacobsen, E. N. *Angew. Chemie - Int. Ed.* **2006**, *45* (10), 1520–1543.
(33) Jeffrey, G. A. *An Introduction to Hydrogen Bonding*; Oxford University Press: New York, 1997.

2.0 Porous Organic Frameworks Catalysts

2.1 Introduction to PAF-1 and PPN-3

As mentioned in chapter 1, we selected PAF-1 as our main framework due to its excellent surface area and its well-established synthesis procedure. Another closely related porous aromatic framework, PPN-3 (**P**orous **P**olymer **N**etwork-**3**), also gained our interest due to its similarity to PAF-1 in term of overall structure and stability, but with a smaller average pore size from the presence of adamantane center instead of the carbon atom (Fig. 4).[1,2] We expected that by working with two frameworks at the same time, the effect of pore size in selectivity can be investigated and compared in greater detail.

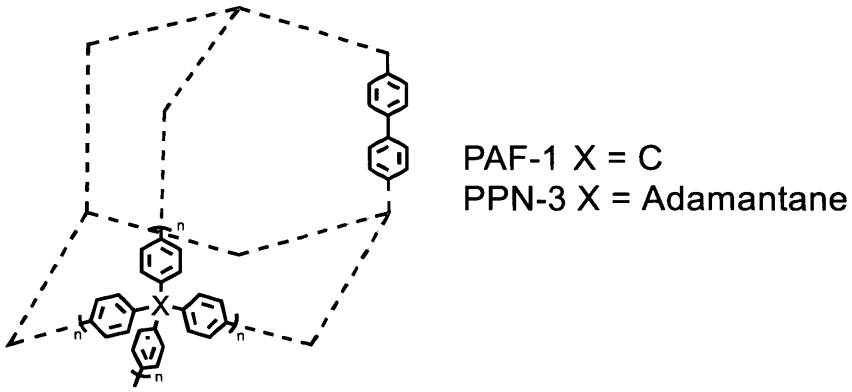

Figure 4. Structure of PAF-1 and PPN-3.

The synthesis of both PAF-1 and PPN-3 are reported in 2009 and 2011 by Ben et al. and Yuan et al. respectively, both using Yamamoto type Ullmann cross-coupling reaction for the polymerization step.[1,3] Yamamoto type Ullmann cross-coupling reaction is an irreversible reaction generally used for aryl halide coupling with bis(1,5-cyclooctadiene)nickel(0) ($Ni(COD)_2$) in excess equivalent as reagent, and is the cross-coupling reaction of choice for PAFs synthesis for its scalability and high efficiency.[4,5] The mechanism of the coupling is shown in Scheme 2 below.[6] The reaction starts with the oxidative reaction of $Ni(COD)_2$ with an aryl halide X–Ar–X monomer. Two complexes of $Ni(COD)_2$ and aryl halides then undergo disproportionation, generating

$Ni(COD)_2X_2$ and $Ni(COD)_2(Ar–X)_2$, which then proceeds via reductive elimination to give X–Ar–Ar–X coupling product that can continue to undergo subsequent reactions. The use of high quality DMF as solvent has also been reported to be crucial to the successful synthesis.[7] Furthermore, a computational study in 2014 by Thomas and Trewin also suggested that DMF might play a role as a template in network formation and prevent network interpenetration during the cross-coupling reaction.[8]

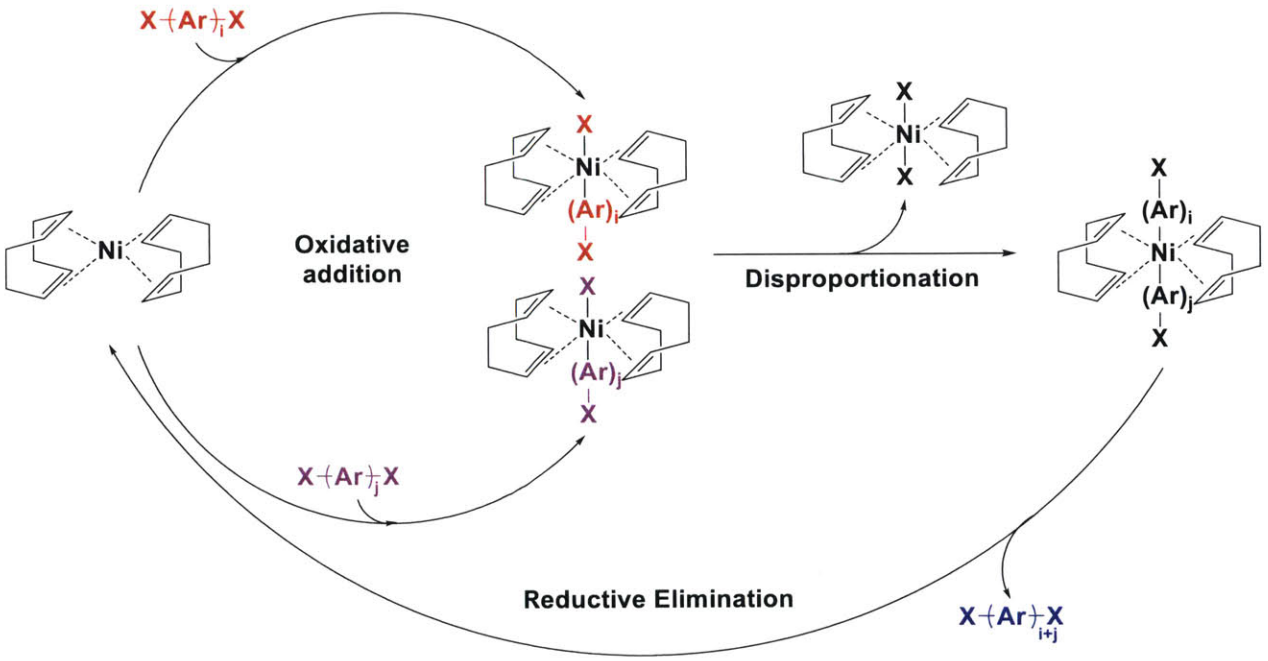

Scheme 2. Mechanism of Yamamoto type Ullman cross-coupling.

Our initial goal was to first verify the synthesis route and obtain PAF-1 and PPN-3 on gram-scale, then ensure their quality via comparison with the reported data (IR spectrum, gas absorption, decomposition, and elemental analysis). After confirmation of the successful synthesis, we would then functionalize these two materials with appropriate functional groups and test their catalytic activity toward aldol reaction in a model reaction. If successful, selectivity and reactivity would be improved by fine-tuning the functionalization.

2.2 Aldol Reaction and Benzoin Condensation

The aldol reaction is one of the most important carbon–carbon bond formation reactions widely found in nature. In biological systems, aldol reaction can be achieved via several routes such as metal enolates or enamine intermediates with help from enzymes.[9] Type I aldolases, the type of enzyme found in animals and plants, facilitate aldol reactions by forming an enamine intermediate from the donor aldehyde or ketone, which then adds to the acceptor aldehyde or ketone, forming the aldol product via the general mechanism shown in Scheme 3.[10]

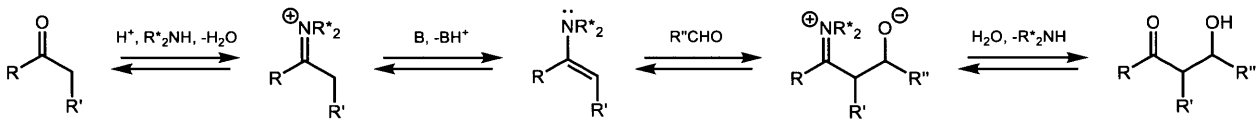

Scheme 3. General mechanism of amine-catalyzed aldol reaction via enamine intermediate.

Other than naturally occurring enzymes, amino acid proline had also been found to catalyze intramolecular aldol reactions from as early as 1971, and was utilized in Woodward's total synthesis of Erythromycin in 1981 and Danishefsky's total synthesis of Taxol in 1996.[11–14] On the other hand, the first proline-catalyzed asymmetric intermolecular aldol reactions were reported by List in 2000.[15] In 1995, it was reported by Reymond et al. that primary and secondary amines were able to catalyze aldol reactions.[16,17] From these reports of the uses of various amines for aldol reactions, we envisioned that we can turn PAFs into size-selective aldol reaction catalysts by attaching appropriate amine groups inside the pore of our materials. As mentioned in Chapter 1 concerning the eventual use of our system for ethanol upgrading, the pore size of PAFs would become the size-selective component of the system that would allow only the transition states of appropriate size to form while preventing the desired product from undergoing further aldol reaction. For this purpose, two simple amines $-NH_2$ and $-CH_2NHMe$, and two amino acids, proline

and glycine, were selected as target functional groups for functionalization of PAFs as aldol reaction catalysts.

Another related reaction that gained our interest was the benzoin condensation reaction, specifically the conversion of ethanol to 1,3-butadiene, an important and valuable building block in many industrial processes.[18] Benzoin condensation is another carbon–carbon bond formation reaction between two aldehyde substrates that proceed via an anion intermediate or an anion equivalent of one aldehyde adding to the second aldehyde.[19] It can be catalyzed by cyanide ions and, as discovered later by Breslow in 1958, *N*-heterocyclic carbene (NHC) catalysts, which were found to be better catalysts than cyanide ions in several aspects.[20,21] We believed that, by introducing NHC group into PAFs, they would act as benzoin condensation reaction catalysts, which we would then be able to investigate their properties using acetaldehyde as substrate with 1,3-butadiene as the final product after further reactions as shown in Scheme 4. This reaction, together with the aldol reaction catalyzed by the amine-functionalized PAFs, would be an interesting starting point for our goal of ethanol upgrading.

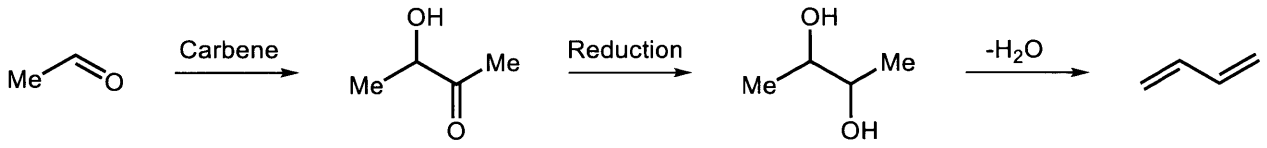

Scheme 4. General scheme for conversion of acetaldehyde to 1,3-butadiene via benzoin condensation.

2.3 Synthesis of PAF-1 and PPN-3

Two main frameworks, PAF-1 and PPN-3 were each synthesized and purified according to existing procedures utilizing nickel-catalyzed Yamamoto type Ullmann cross-coupling reaction in three steps.[1,7] The synthesis was successful with overall yields of 32% and 13% for PAF-1 and PPN-3 respectively (Scheme 5).

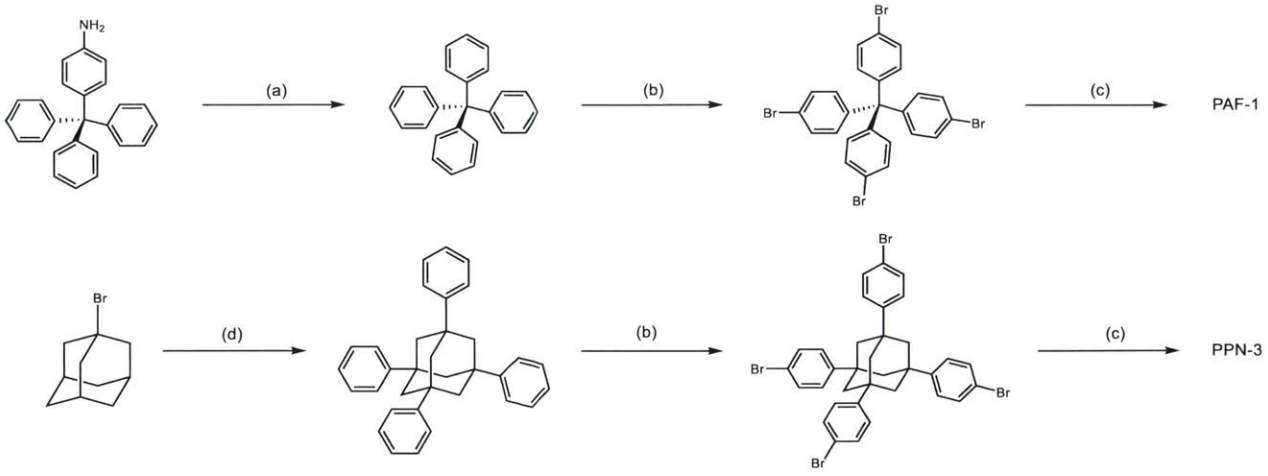

Scheme 5. Synthetic route of PAF-1 and PPN-3. Reagent and conditions: a) 4-tritylaniline, isoamylnitrite, H_2SO_4, $H_4P_2O_6$, DMF, 50 °C; b) Br_2, –78 °C to rt, 18 h; c) $Ni(COD)_2$, 2,2'-bipyridyl, DMF, 72 h, 80 °C, then conc. HCl, 48 h, rt; d) benzene, t-butyl iodide, $AlCl_3$, 12 h, 90 °C.

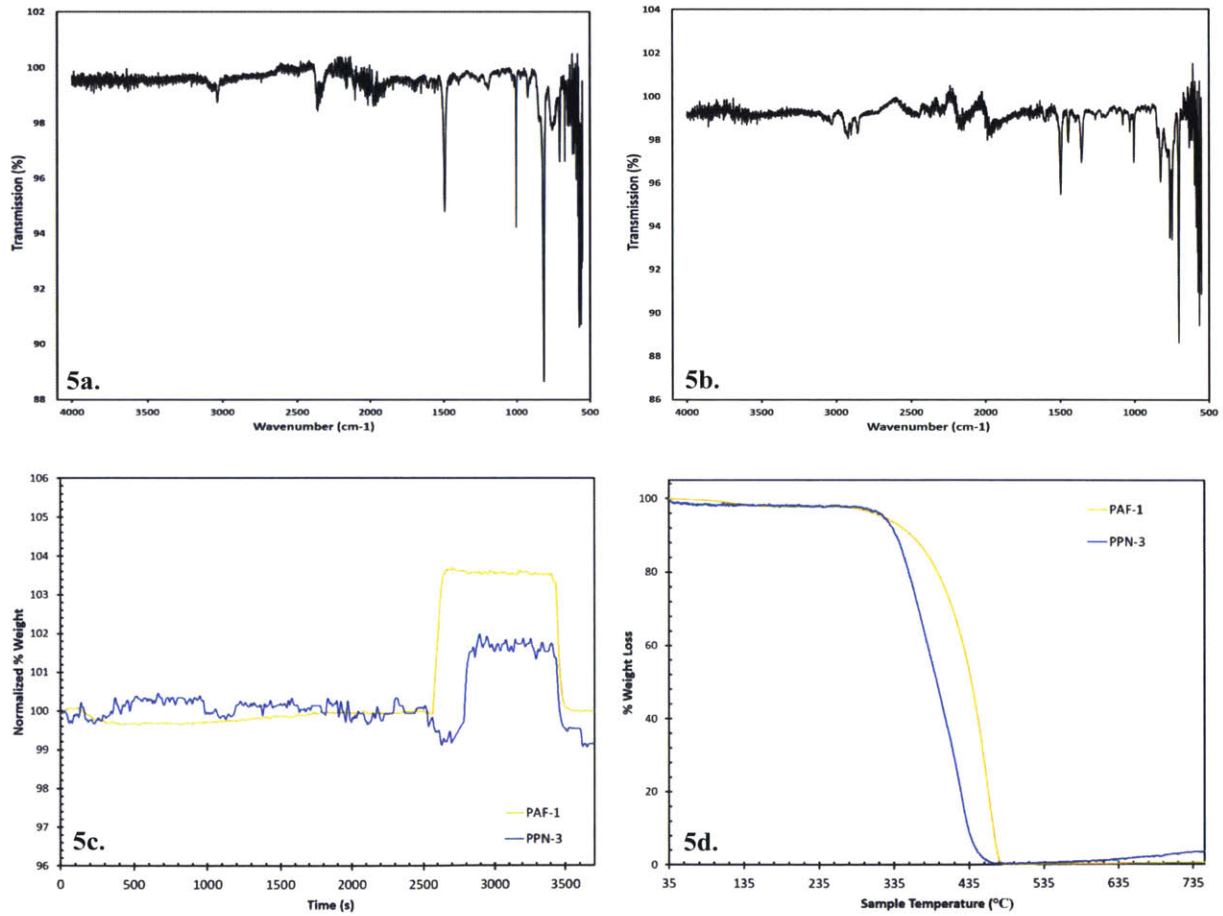

Figure 5. a) IR spectrum of PAF-1; b) IR spectrum of PPN-3; c) CO_2 absorption of PAF-1 and PPN-3; d) Decomposition profile of PAF-1 and PPN-3.

Although the yields were less than optimal, we were able to obtain enough of both materials for initial characterization and subsequent reactions. Shown in Figure 5 are the IR spectrum, CO_2 absorption, and decomposition profiles of PAF-1 and PPN-3. Gas absorption is a useful method for characterization of porous materials since gas uptake capacity is proportional to the material's surface area and surface chemistry, which tells us about overall structure of material. Full characterization data of PAF-1 and PPN-3 can be found in the supporting information (SI).

2.4 Functionalization of PAF-1 and PPN-3

After PAF-1 and PPN-3 had been successfully obtained, we aimed to first functionalize them with simple amine groups where existing synthesis procedures are known, specifically $-NH_2$ and $-CH_2NHMe$ (Scheme 6).[7,22] We expected that these amine groups would be able to catalyze aldol reactions via enamine intermediates as mentioned in Chapter 2.2. Since it was unknown to us what percentage of the framework should be functionalized for optimal catalytic activity and selectivity, we decided to use excess amount of reagents to fully functionalize our materials as a starting point. As a result, four different materials (PAF-1-NH_2, PAF-1-CH_2NHMe, PPN-3-NH_2, and PPN-3-CH_2NHMe) were synthesized according to literature, and were characterized with IR and TGA. Full characterization data can be found in Supporting Information (SI).

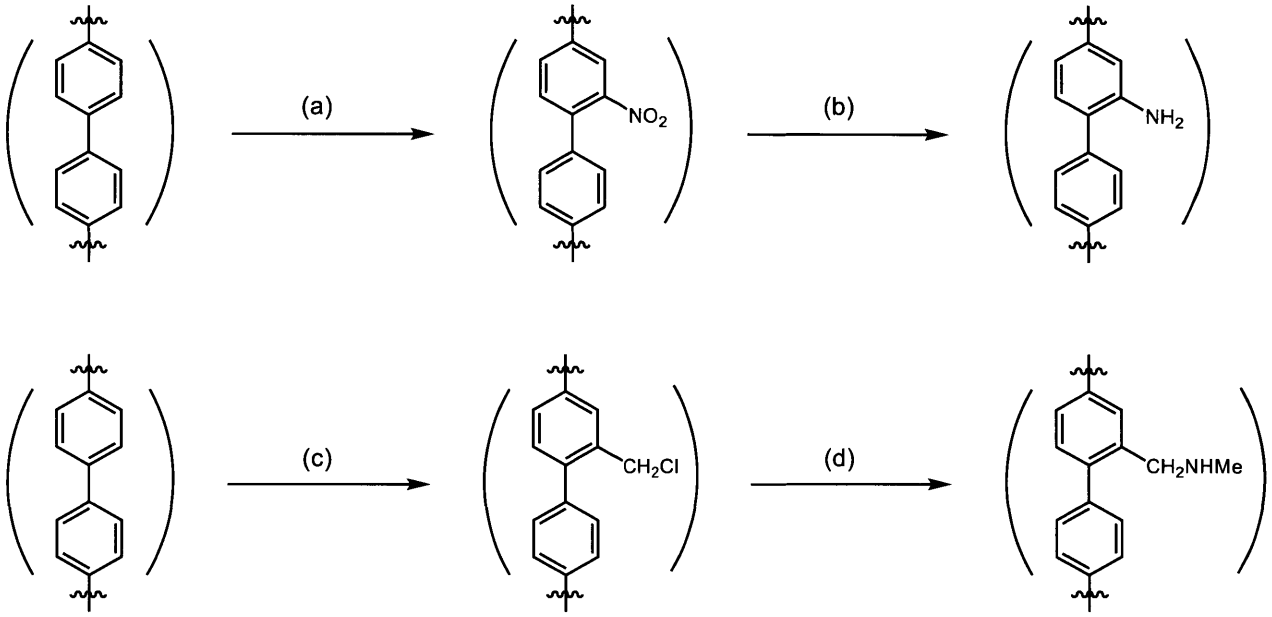

Scheme 6. Synthetic route of $-NH_2$ and $-CH_2NHMe$ PAFs. Reagent and conditions: a) $Cu(NO_3)_2 \cdot 2.5H_2O$, acetic anhydride, CH_2Cl_2, 0 °C to rt, 24 h; b) $Na_2S_2O_4$, 70 °C, 24 h; c) paraformaldehyde, HCl, H_3PO_4, AcOH, 90 °C, 72 h; d) methylamine solution, 80 °C, 72 h.

Shown in Figure 6 are thermogravimetric analysis data for carbon dioxide absorption and decomposition profiles of the functionalized materials in comparison to those of original PAF-1 and PPN-3. In the absorption experiment, each material was first heat in nitrogen atmosphere to remove solvent traces, which resulted in weight loss observed at the beginning. The material was allowed to cool down slowly under nitrogen atmosphere, then put under carbon dioxide atmosphere, and back to nitrogen atmosphere. As expected, the presence of CO_2-philic $-NH_2$ group increases CO_2 absorption for both PAF-1 and PPN-3. However, when the larger $-CH_2NHMe$ group is added, the changes in CO_2 absorption are inconsistent, possibly due to different pore sizes and structures between PAF-1 and PPN-3. In term of thermal stability, functionalized PAFs started decomposing at slightly lower temperature ranges than those of PAF-1 and PPN-3, but were still stable at temperature up to approximately 350 °C in most cases.

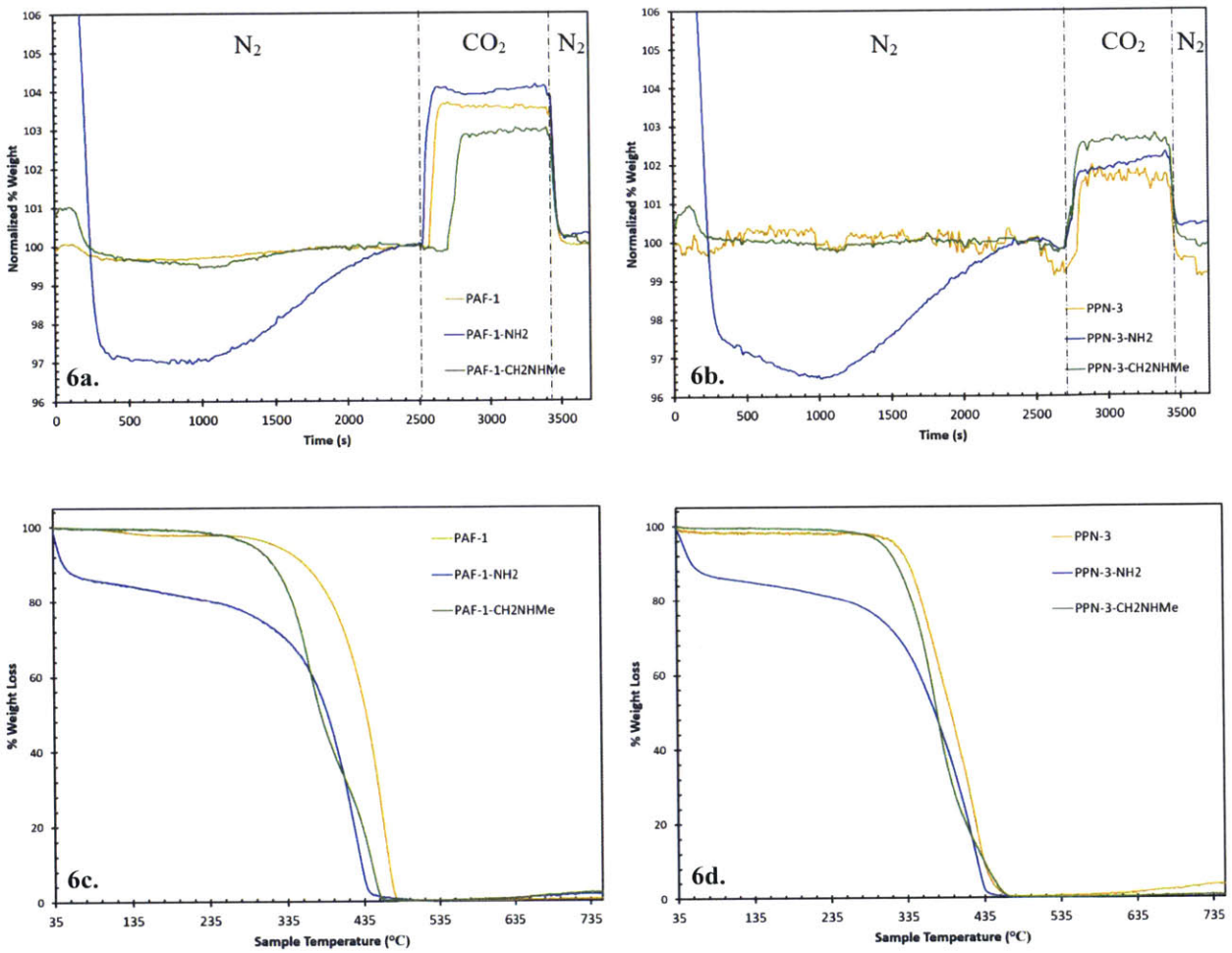

Figure 6. TGA data. a) CO_2 absorption of PAF-1 and its derivatives; b) CO_2 absorption of PPN-3 and its derivatives; c) Decomposition profile of PAF-1 and its derivatives; d) Decomposition profile of PPN-3 and its derivatives.

Other than simple linear amine groups, other functional groups discussed earlier were incorporated into PAFS. These include amino acids proline and glycine, which were selected with our expectation that the extra functional group on these groups would lead to different selectivity and reactivity. 1-Methylimidazole was also selected to be incorporated into our framework to create a *N*-heterocyclic carbene catalyst for the benzoin condensation reaction. The synthetic scheme of these materials are shown below in Scheme 7, and their corresponding TGA data are in Figure 7. Note that only PAF-1 was selected for these specific functionalization.

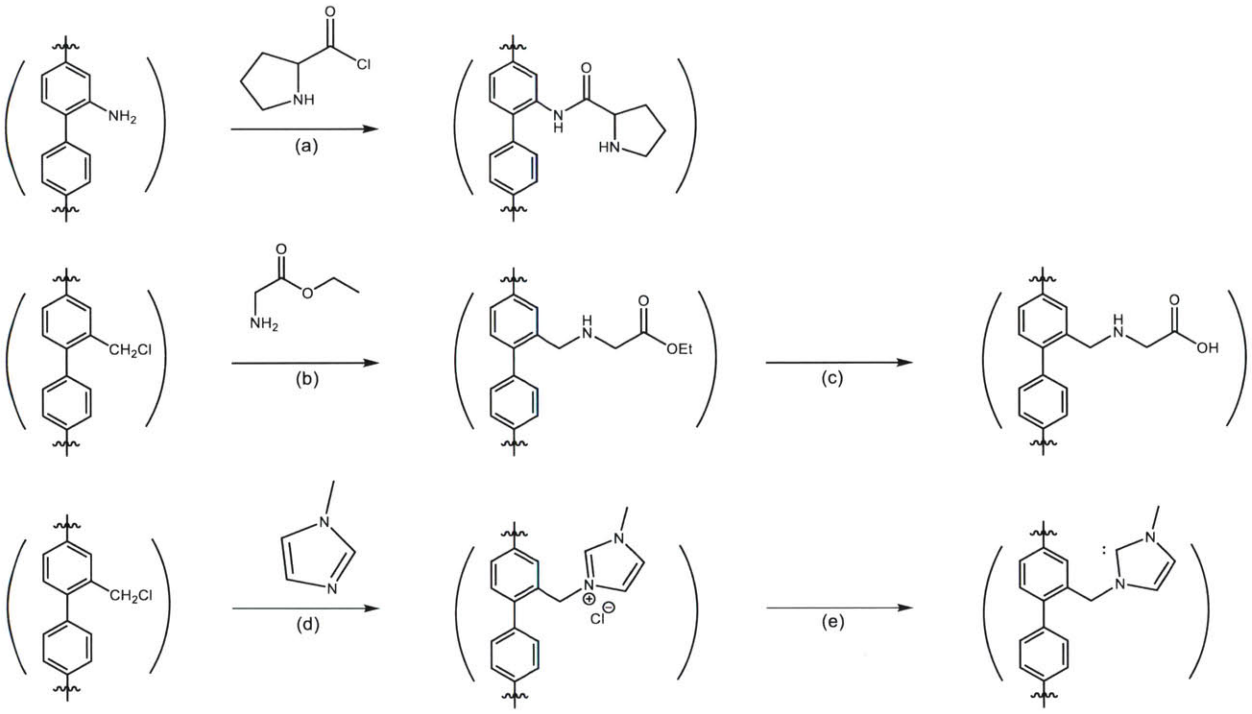

Scheme 7. Synthetic route of functionalized PAFs. Reagent and conditions: a) proline acid chloride, THF, rt, 24h; b) glycine ethyl ester hydrochloride, Et_3N, PhMe, 80 °C, 24 h; c) H_2O; d) 1-methylimidazole, PhMe, 65 °C, 24 h; e) t-BuOK, THF, rt, 48 h.

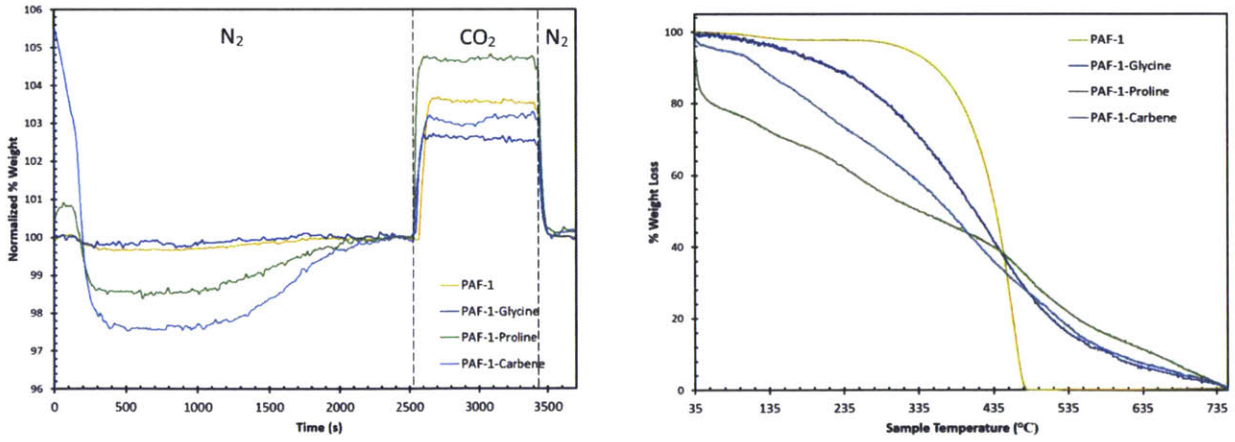

Figure 7. TGA data. a) CO_2 absorption of PAF-1 and its derivatives; b) Decomposition profile of PAF-1 and its derivatives.

2.5 Reactivity for Aldol Reaction and Benzoin Condensation

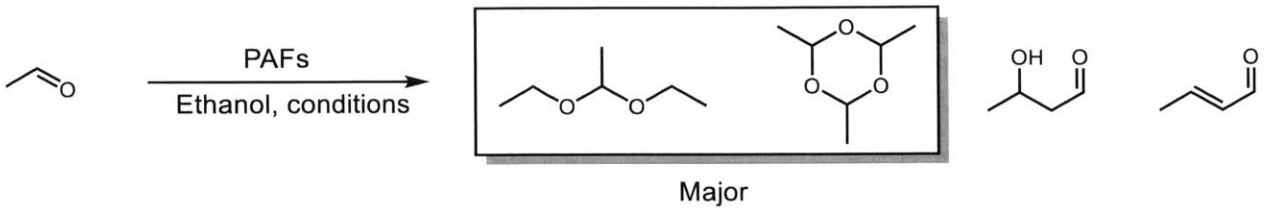

Scheme 8. Model reaction for reactivity of PAF catalysts for aldol reaction.

Butyraldehyde, acetaldehyde, and ethanol were selected as model substrates and solvent to test catalytic activity of amine- and amino acid-functionalized PAFs for aldol reactions (Scheme 8). In each experiment, a small amount of PAFs was put in ethanol solvent, then the aldehyde was added to the reaction. After a specific reaction time, a small aliquot of the reaction mixture was filtered through a Pasteur pipette filled with cotton plug and Celite to remove any solid particle. The filtered sample was then characterized with gas chromatography with flame ionization detector (GC-FID). Unfortunately, results from gas chromatography indicated no formation of the aldol product from any reaction conditions we tried. Instead, linear and cyclic acetals were found to be the only major products where the exact acetal depended on the aldehyde and alcohol solvent used. Similarly, the test for benzoin condensation catalyzed by PAF-NHC also proved to be unsuccessful, with no formation of the desire product as determined by GC-FID.

The undesired reactivity of our framework catalysts was a surprise to us since we initially expected high reactivity from most catalysts, and that selectivity was to be the main focus of our work. We suspected that the products were unable to exit the framework as freely as expected, which was supported by the work of another graduate student in our group that showed little substrate diffusion in a comparable system.[23] We eventually decided to end this project due to the lack of promising result and the better prospect of using another type of catalytic system.

References

(1) Yuan, D.; Lu, W.; Zhao, D.; Zhou, H.-C. *Adv. Mater.* **2011**, *23* (32), 3723–3725.

(2) Lu, W.; Yuan, D.; Zhao, D.; Schilling, C. I.; Plietzsch, O.; Muller, T.; Bräse, S.; Guenther, J.; Blümel, J.; Krishna, R.; Li, Z.; Zhou, H.-C. *Chem. Mater.* **2010**, *22* (21), 5964–5972.

(3) Ben, T.; Ren, H.; Ma, S.; Cao, D.; Lan, J.; Jing, X.; Wang, W.; Xu, J.; Deng, F.; Simmons, J. M.; Qiu, S.; Zhu, G. *Angew. Chemie - Int. Ed.* **2009**, *48* (50), 9621–9624.

(4) Kizzie, A. C.; Dailly, A.; Perry, L.; Lail, M. A.; Lu, W.; Nelson, T. O.; Cai, M.; Zhou, H. *Mater. Sci. Appl.* **2014**, *05* (06), 387–394.

(5) Lu, W.; Wei, Z.; Yuan, D.; Tian, J.; Fordham, S.; Zhou, H. C. *Chem. Mater.* **2014**, *26*, 4589–4597.

(6) Ben, T.; Qiu, S. *CrystEngComm* **2013**, *15* (1), 17–26.

(7) Van Humbeck, J. F.; McDonald, T. M.; Jing, X.; Wiers, B. M.; Zhu, G.; Long, J. R. *J. Am. Chem. Soc.* **2014**, *136* (6), 2432–2440.

(8) Thomas, J. M. H.; Trewin, A. *J. Phys. Chem. C* **2014**, *118* (34), 19712–19722.

(9) Machajewski, T. D.; Wong, C.-H. *Angew. Chemie Int. Ed.* **2000**, *39* (8), 1352–1375.

(10) Bahmanyar, S.; Houk, K. N. *J. Am. Chem. Soc.* **2001**, *123* (45), 11273–11283.

(11) Woodward, R. B.; Logusch, E.; Nambiar, K. P.; Sakan, K.; Ward, D. E.; Auyeung, B. W.; Balaram, P.; Browne, L. J.; Card, P. J.; Chen, C. H.; Chenevert, R. B.; Fliri, a; Frobel, K.; Gais, H. J.; Garratt, D. G.; Hayakawa, K.; Heggie, W.; Hesson, D. P.; Hoppe, D.; Hoppe, I.; Hyatt, J. a; Ikeda, D.; Jacobi, P. a; Kim, K. S.; Kobuke, Y.; Kojima, K.; Krowicki, K.; Lee, V. J.; Leutert, T.; Malchenko, S.; Martens, J.; Matthews, R. S.; Ong, B. S.; Press, J. B.; Rajanbabu, T. V; Rousseau, G.; Sauter, H. M.; Suzuki, M.; Tatsuta, K.; Tolbert, L. M.; Truesdale, E. a; Uchida, I.; Ueda, Y.; Uyehara, T.; Vasella, a T.; Vladuchick, W. C.; Wade, P. a; Williams, R. M.; Wong, H. N. C. *J. Am. Chem. Soc.* **1981**, *103* (11), 3210–3213.

(12) Danishefsky, S. J.; Danishefsky, S. J.; Masters, J. J.; Masters, J. J.; Young, W. B.; Young, W. B.; Link, J. T.; Link, J. T.; Snyder, L. B.; Snyder, L. B.; Magee, T. V; Magee, T. V; Jung, D. K.; Jung, D. K.; Isaacs, R. C. a; Isaacs, R. C. a; Bornmann, W. G.; Bornmann, W. G.; Alaimo, C. a; Alaimo, C. a; Coburn, C. a; Coburn, C. a; Di Grandi, M. J.; Di Grandi, M. J. *J. Am. Chem. Soc.* **1996**, *118* (12), 2843–2859.

(13) Eder, U.; Sauer, G.; Wiechert, R. *Angew. Chemie Int. Ed.* **1971**, *10* (1958), 496–497.

(14) Hajos, Z. G.; Parrish, D. R. *J. Org. Chem.* **1974**, *39* (12), 1615–1621.

(15) List, B.; Lerner, R. a; Iii, C. F. B.; Torrey, N.; Road, P.; Jolla, L.; December, R. V. *J. Am. Chem. Soc.* **2000**, *122* (13), 2395–2396.

(16) Reymond, J.-L.; Chen, Y. *J. Org. Chem.* **1995**, *60* (21), 6970–6979.

(17) Reymond, J.-L. *J. Mol. Catal. B Enzym.* **1998**, *5* (1-4), 331–337.

(18) Jones, M. D. *Chem. Cent. J.* **2014**, *8*, 1–5.

(19) Kankala, S.; Edulla, R.; Modem, S.; Vadde, R.; Vasam, C. S. *Tetrahedron Lett.* **2011**, *52* (29), 3828–3831.

(20) Wöhler; Liebig. *Ann. der Pharm.* **1832**, *3* (3), 249–282.

(21) Breslow, R. *J. Am. Chem. Soc.* **1958**, *80* (14), 3719–3726.

(22) Lu, W.; Sculley, J. P.; Yuan, D.; Krishna, R.; Wei, Z.; Zhou, H.-C. *Angew. Chemie - Int. Ed.* **2012**, *124* (30), 7480–7484.

(23) Palmer, R. D. Mass Transport in Metal-Organic Frameworks As a Limiting Step in Size-Selective Oligomerization, Massachusetts Institute of Technology, 2016.

3.0 C3-Symmetric Receptor Catalysts

3.1 Synthesis of non-Fluorinated Receptors

Based on the established precursor, 1,3,5-tris(bromomethyl)-2,4,6-triethylbenzene **1**, which was described previously in the introduction, we came up with our original catalyst design **2a** shown below in Figure 8.[1]

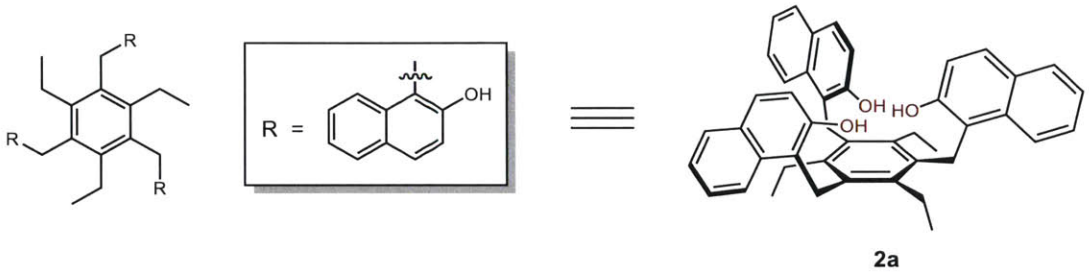

2a

Figure 8. The original design of C3-symmetric receptor catalyst with three naphthol arms.

This catalyst design features three 2-naphthol groups alternating with three ethyl groups. We expected that our structure would assume the *ababab* conformation with all ethyl groups facing toward one face and the three naphthol groups facing toward the opposite face similar to what have been reported for other receptors based on the same precursor.[2–4] We also expected that the large size of naphthyl groups would be bulky enough to gear the three hydroxyl groups toward the center of the structure, forming a hydrogen bond "pocket". The position and orientation of hydroxyl groups deep inside the pocket would prevent binding with H-bond acceptors that are too bulky or do not have appropriate shape and size, which would facilitate regioselective catalysis.

The synthesis of this catalyst is shown in Scheme 9 which begins with preparation of 1,3,5-tris (bromomethyl)-2,4,6-triethylbenzene **1** from 2,4,6-triethylbenzene **3** from a known procedure followed by copper-catalyzed Grignard reaction between **1** and 1-bromo-2-methoxynaphthalene which yielded **4** as white solid.[1] However, **4** was found to have very limited solubility in common

solvents, only soluble in chloroform at high temperature. We suspected that this low solubility was perhaps due to the rigidity of the structure since peak broadenings were observed in the ^{1}H NMR spectrum and broadening can indicate limited mobility of bond rotation. This low solubility unfortunately forbade us from obtaining the desired catalyst **2a**.

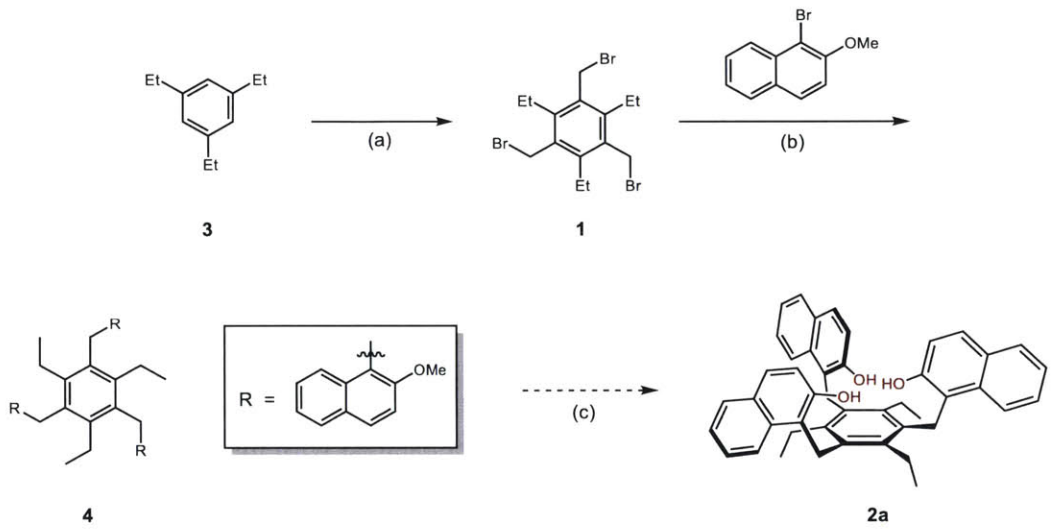

Scheme 9. Synthetic route of the original C3-symmetric receptor catalyst **2a**. Reagent and conditions: a) paraformaldehyde, $ZnBr_2$, HBr/AcOH, 90 °C, 18 h; b) Mg activated by I_2, CuI, THF, 55 °C, 18 h; c) BBr_3, DCM, 0 °C, 4 h.

Since the low solubility would make the use of our catalyst impractical for most common chemical reactions, we proposed several modifications to **2a** that would incorporate long and flexible alkyl chains to the catalyst to improve solubility (Figure 9). Catalyst **2b** replaces the three ethyl groups with longer butyl groups while catalysts **2c** and **2d** add alkyl chain to the naphthol part of the catalyst. While the synthesis of **2b** and **2c** were found to proceed in very low yields, the synthesis of **2d** via Suzuki Coupling, copper-catalyzed Grignard reaction, followed by demethylation using boron tribromide, proceeds in yields high enough for gram-scale synthesis (Scheme 10). **2d** was also found to have good solubility in common polar solvents as we hoped. The properties and reactivity of **2d** is further discussed in section 3.3 and section 3.4.

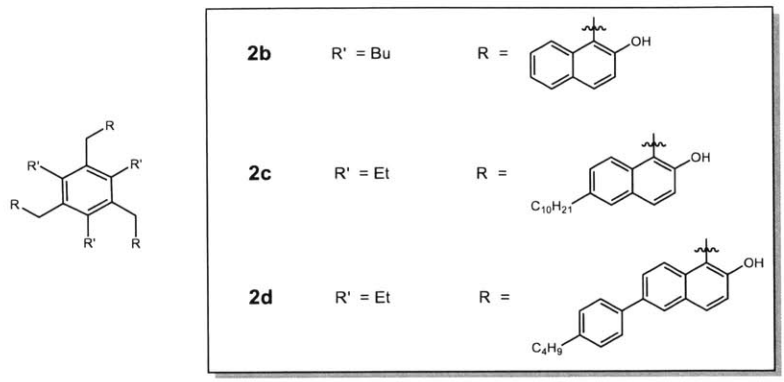

Figure 9. Proposed modifications to the original design of C3-symmetric receptor catalyst to improve solubility (**2b-d**).

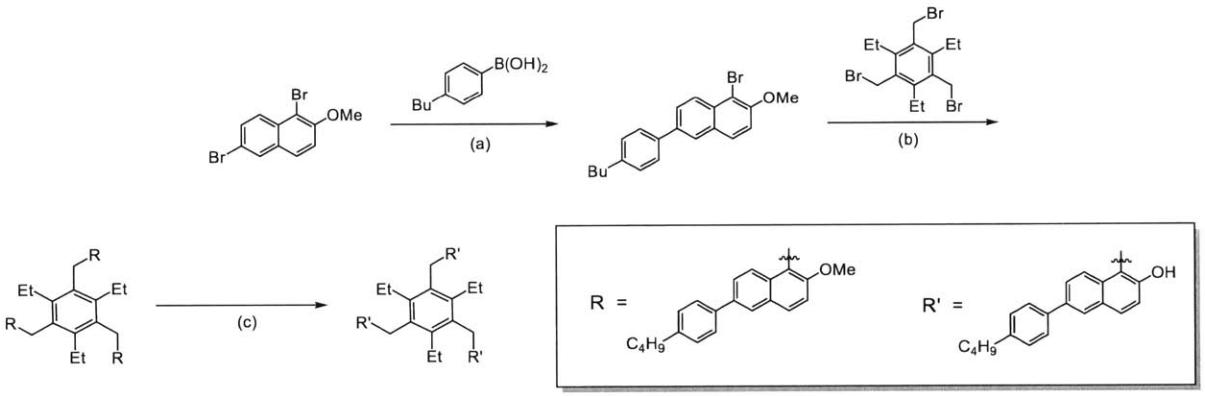

Scheme 10. Synthetic route of modified catalyst **2d**. Reagent and conditions: a) $Pd(PPh_3)_4$, K_2CO_3, H_2O / PhMe / MeOH, 80 °C, 18 h; b) Mg activated by I_2, CuI, THF, 55 °C, 18 h; c) BBr_3, DCM, 0 °C, 4 h.

3.2 Attempted Synthesis of Fluorinated Receptors

After the successful synthesis of catalyst **2d**, we began to explore the modification that would further improve the catalyst's binding and reactivity. One possible method is to increase the acidity of hydroxyl groups by replacing naphthyl hydrogen with fluorine, which is a better electron-withdrawing group than hydrogen. After comparing several potential methods for fluorinating the naphol group, we decided to base our design on the procedure for the synthesis of 5-bromo-1,2,3,4-tetrafluoro-6-methoxy naphthalene **5** via Diels-Alder reaction of benzyne, which was originally reported as an intermediate for the synthesis of fluorinated BINOL (F_8BINOL).[5]

Structure **5** was decided to be suitable for incorporation into our catalyst design since it features structure compatible with our established synthetic route of **2d**. Structure **6** was then proposed as our modified catalysts based on this fluorinated naphthol precursor.

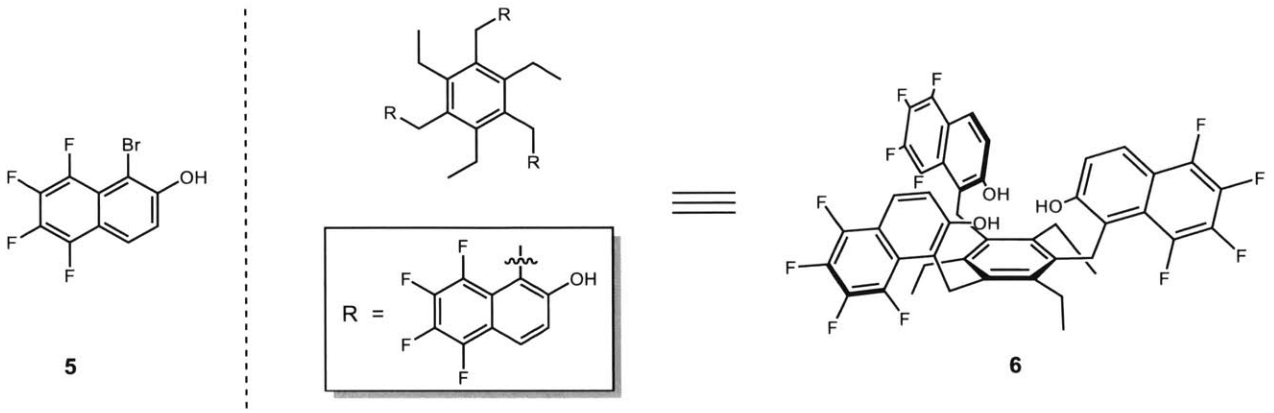

Figure 10. Proposed structure of fluorinated receptor catalyst.

We first attempted to perform copper-catalyzed Grignard reaction between **7** and 1,3,5-tris(bromomethyl)-2,4,6-triethylbenzene to obtain methoxy-protected tripodal receptor **8** in a similar manner to our previous synthesis of **2a-d** (Scheme 11). We were initially unable to form the Grignard reagent of **7** when iodine was used for magnesium activation, but later found that the Grignard reagent can be formed in good yield if dibromoethane was used for magnesium activation instead.[6] However, although the Grignard reagent was formed, we did not observe any C–C bond formation between the naphtyl Grignard and 1,3,5-tris(bromomethyl)-2,4,6-triethylbenzene. We then used *n*-butyllithium to generate organolithium reagent of **7**, but again did not observe formation of the desired product. An alternative route where the C–C bond formation between 1,3,5-tris(bromomethyl)-2,4,6-triethylbenzene and 3-methoxythiophene was made first followed by the Diels-Alder reaction with chloropentafluorobenzene was not successful either. We concluded that the organolithium reagent and Grignard reagent of **7** might not be reactive enough

to give a successful SN_2 coupling reaction under our current reaction conditions. We then decided to stop pursuing this target structure and proceeded with the non-fluorinated receptor.

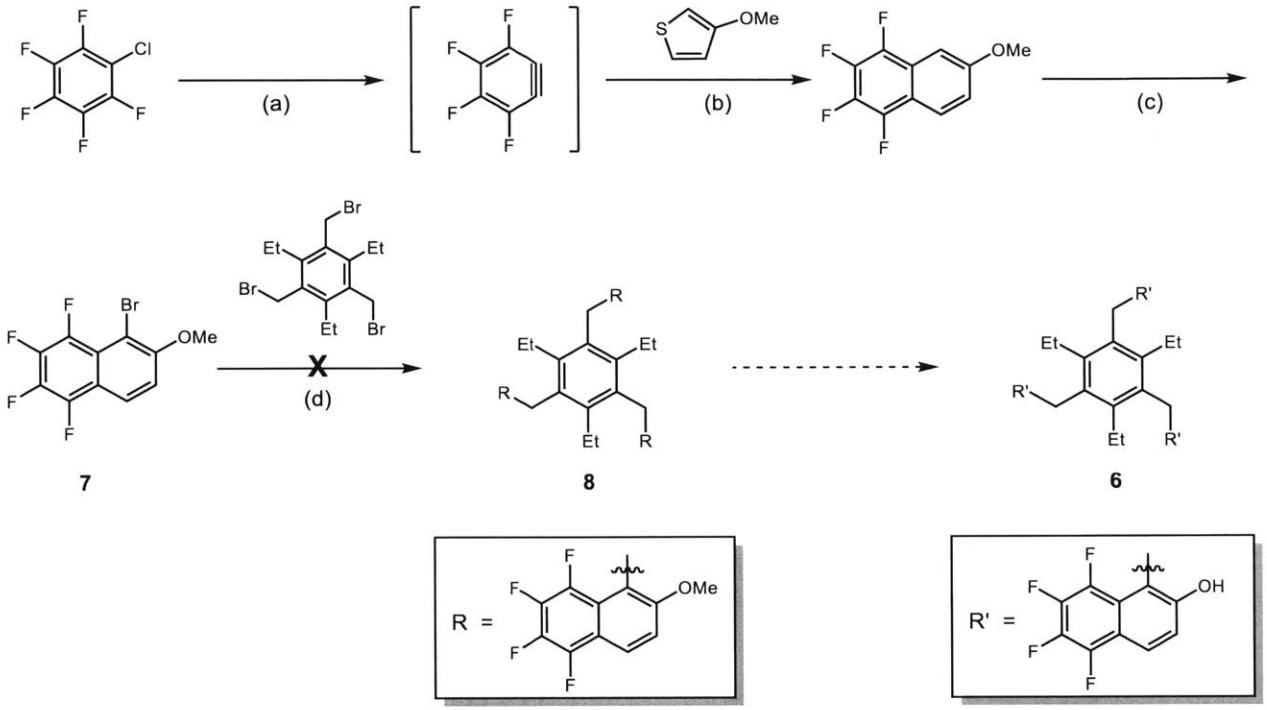

Scheme 11. Proposed synthetic route of fluorinated receptor catalyst **6**. Reagent and conditions: a) *n*-BuLi, hexane, –15 °C; b) –15 °C to rt, 12 h; c) NBS, CH_3CN, rt, 1 h; d) Mg, CuI, 12 h, 55 °C.

3.3 Binding Studies of C3-Symmetric Receptor

In order to measure and quantify the interaction between our catalyst and substrate molecule, we chose to perform an NMR titration experiment. Titration experiments are a common method in the field of supramolecular chemistry that can be used to quantitatively measure interaction between the host (usually the larger molecule) and the guest (the smaller molecule) by measuring the change in a physical property of the system such as the NMR or UV spectrum while the ratio between the host and the guest is changing. The data can then be plotted and analyzed with appropriate binding model and regression method.[7]

In our case, we kept the concentration of our host (the C3-symmetric receptor **6**) constant while changing the concentration of our substrate molecule in the range of 0.1 to 21.6 equivalent of the host (See Supporting Information for complete experimental procedure). Five different substrates with various functional groups and types were selected for the binding studies. The results were analyzed using a Matlab-based analysis program (*fittingprogram*) written by Lowe, Pfeffer, and Thordarson in 2012.[8] From this program, binding constants K_a and associated uncertainties were calculated. We assumed that our system is a simple 1:1 binding, and two sets of proton NMR shifts or isotherms were used for each calculation ('global' data analysis). The results are shown below in Table 1 and Figure 11.

Guest Substrate	Binding Constant K_a
n-butanol	no binding (< 10 M^{-1})
sec-butanol	13.3 M^{-1} (± 217%)
n-butylamine	165.0 M^{-1} (± 37%)
sec-butylamine	101.9 M^{-1} (± 42%)
n-butyric acid	1886.5 M^{-1} (± 201%)

Table 1. Calculated binding constant K_a for 1:1 binding equilibria from ^1H NMR titrations of a range of substrates and C3-symmetric receptor.

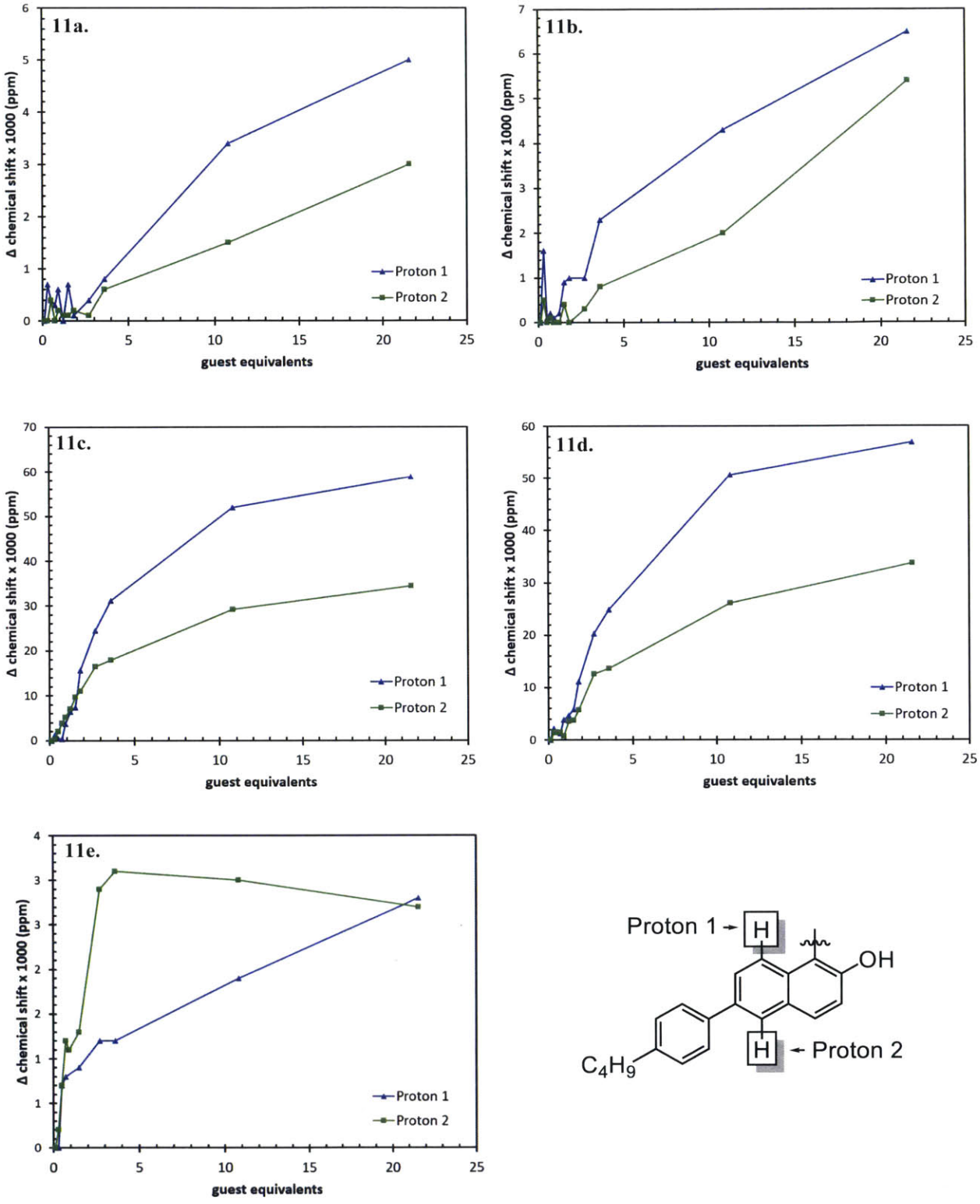

Figure 11. ^{1}H NMR binding isotherms from the titration of C3-symmetric receptor and various substrates. a) n-butanol; b) sec-butanol; c) n-butylamine; d) sec-butylamine; e) n-butyric acid.

The results shown in Table 1 and Figure 11 suggests that although our receptor system binds to these hydrogen-bond acceptors, the bindings are still relatively weak with most binding constants in the range of less than 1000 M^{-1} while reported binding constants for other systems are usually between 10^3 to 10^5 for strong bindings.[7–9] While the K_a value for the amine bindings was larger than those for alcohol bindings as expected, it was a surprise to us that K_a value for the carboxylic acid binding was the largest. However, it is possible that the high binding constant for the carboxylic acid binding could have been caused by experimental uncertainties since the chemical shift differences observed for the carboxylic acid binding were very small ($3x10^{-3}$ ppm for the largest difference), which resulted in the plot shape being irregular (Figure 11e). The low binding interactions between the receptor and alcohol substrates, n-butanol and sec-butanol, led to small K_a values with very high uncertainties and irregular shaped plots, making the comparison between the two unreliable. Nevertheless, in the case of the two amines, n-butylamine and sec-butylamine, the binding constants K_a were sufficiently high enough with acceptable uncertainties (165.0 M^{-1} (± 37%) and 101.9 M^{-1} (± 42%) respectively). In this case, our receptor shows a slight preference toward binding to n-butylamine, which supports our expectation that the receptor would preferentially bind to the more accessible hydrogen-bond acceptor due to the pocket-shape structure of our receptor. However, since pK_a of n-butylamine is slightly higher than that of sec-butylamine (10.8 and 10.56 respectively), the preference toward n-butylamine might be partly caused by the inherent nature of n-butylamine as a better hydrogen-bond acceptor.[10] It should also be noted that K_a values of the two amines are within the uncertainty range of each other.

3.4 Catalytic Properties of C3-Symmetric Receptor

After the data from the NMR titration experiment were obtained, a range of nucleophiles, electrophiles, and solvents was selected for a high-throughput screening (Scheme 12). The high-

throughput screening method would allow us to quickly identify potential substrate pairs and also possibly identify new transformation or reaction pathway that was not expected.[11] The decision for our substrates and solvents was done in consideration to the expected reaction temperature, appropriate binding activities, and a range of nucleophilicity. Solvent choices were limited to those that are relatively polar due to solubility of the receptor. Each sample from each reaction was characterized with GC-FID and compared to referenced standard peaks. We then looked for the result of the substrate pairs that produced new peaks with significant peak area that have higher retention time than our starting materials and compared the relative yields of the reaction with catalyst to those without catalyst. Substrate pairs that produced no new product or those where the presence of the catalyst did not make a difference were disregarded.

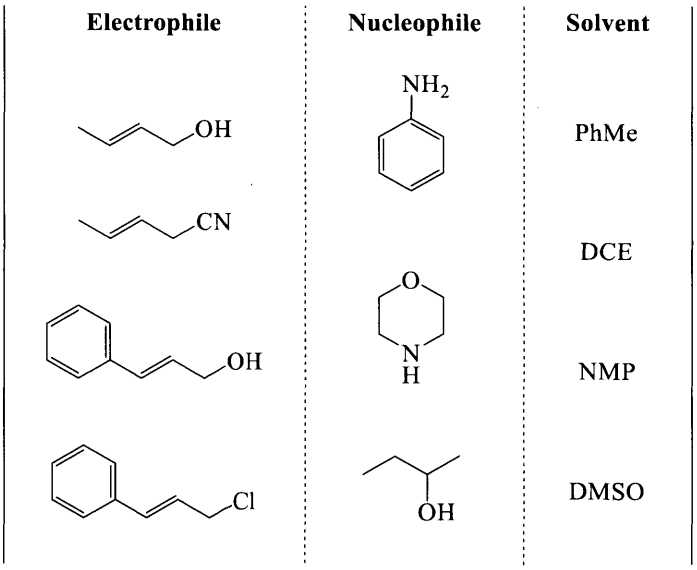

Scheme 12. Substrates and solvents selected for the high-throughput screening. Reaction conditions: 1:1 electrophile to nucleophile, catalyst 5% mol, 80 °C, 12 h. No catalyst for controlled reactions.

After two screenings, cinnamyl chloride and aniline were identified as a potential model substrate pair. With the aid of our catalyst, cinnamyl chloride reacts with aniline via what appears to be S_N2 reaction with an improved yield of 20% compared to 7% without the catalyst when N-Methyl-2-pyrrolidone (NMP) was used as solvent. Other substrate pairs showed either no or

similar reactivity with and without the catalyst. Starting from this knowledge, we proceeded to optimize this reaction by changing a number of parameters of the reaction. A range of solvents were screened and DMF was found to give a slightly better result than NMP.

At first we suspected that the low yield might be caused by inhibition of the catalyst from chloride ions that were released from cinnamyl chloride from the S_N2 reaction. Since binding between receptors and chloride ions is expected to be stronger than binding between receptors and substrates, as chloride ions are generated, the receptor will be occupied by chloride and unable to bind with unreacted substrates.[12–14] We hope that by using bicarbonate salt, chloride ions would be removed from the catalyst, freeing it for further catalysis. However, we found that while the addition of sodium bicarbonate and other salts helped improve the yield, the yields of background reaction (reaction without catalyst) in these cases also increased, resulting in only a small difference in yields between reactions with and without the catalyst. Similar results were also obtained when bulky organic bases including 1,8-bis(dimethylamino)naphthalene, 2,6-Lutidine, and DABCO were used as additive instead of inorganic salts. Attempts to decrease background reaction by lowering reaction temperature did not yield satisfactory result as the reactivity of the catalyst also decreased.

References

(1) Walsdorff, Christian; Saak, Wolfgang; Pohl, S. *J. Chem. Res. Synopses* **1996**, No. 6, 282–283.

(2) Dell'Anna, G. M.; Annunziata, R.; Benaglia, M.; Celentano, G.; Cozzi, F.; Francesconi, O.; Roelens, S. *Org. Biomol. Chem.* **2009**, *7* (18), 3871–3877.

(3) Chin, J.; Walsdorff, C.; Stranix, B.; Oh, J.; Chung, H. J.; Park, S. M.; Kim, K. *Angew. Chemie - Int. Ed.* **1999**, *38* (18), 2756–2759.

(4) Cacciarini, M.; Cordiano, E.; Nativi, C.; Roelens, S. *J. Org. Chem.* **2007**, *72* (10), 3933–3936.

(5) Yudin, A. K.; Martyn, L. J. P.; Pandiaraju, S.; Zheng, J.; Lough, A. *Org. Lett.* **2000**, *2* (1), 41–44.

(6) Huo, S. *Org. Lett.* **2003**, *5* (4), 423–425.

(7) Thordarson, P. *Chem. Soc. Rev.* **2011**, *40* (3), 1305–1323.

(8) Lowe, A. J.; Pfeffer, F. M.; Thordarson, P. *Supramol. Chem.* **2012**, *24* (8), 585–594.
(9) Dethlefs, C.; Eckelmann, J.; Kobarg, H.; Weyrich, T.; Brammer, S.; Näther, C.; Lüning, U. *European J. Org. Chem.* **2011**, *2011* (11), 2066–2074.
(10) Perrin, D. D. *Pure Appl. Chem.* **1969**, *20* (2), 133–236.
(11) McNally, A.; Prier, C. K.; MacMillan, D. W. C. *Science (80-.).* **2011**, *334* (6059), 1114–1117.
(12) Metz, A. E.; Ramalingam, K.; Kozlowski, M. C. *Tetrahedron Lett.* **2015**, *56* (37), 5180–5184.
(13) Turner, D. R.; Paterson, M. J.; Steed, J. W. *J. Org. Chem.* **2006**, *71* (4), 1598–1608.
(14) Fukawa, M.; Sato, T.; Kabe, Y. *Chem. Commun.* **2015**, *51* (79), 14746–14749.

4.0 Discussion

Porous aromatic frameworks or PAFS have been established as novel material with impressive properties which led to various useful applications especially in the field of small molecule recognition and gas storage.[1,2] However, from the low reactivity that we observed from our systems, it appears that PAFs, or at least PAF-1 and PPN-3, may not be a suitable platform for catalysis until there is a better understanding of PAFs structure. However, since there are examples of using PAFs in catalysis, such as the work from the Sánchez group and the Ma group, we suspected that our unsuccessful results might be from either our choice of PAFs, the catalytic functional groups, or the nature of our substrates and reaction condition.[3–6] It was suggested by the work of another graduate student in our group that mass transport or the process of the substrate and product diffusing in and out of the material could be the limiting factor in catalysis in porous materials.[7] The work from the Sanchez group, for example, employed PAFs that have larger pore sizes and pore aperture sizes than those of PAF-1 and PPN-3, which means that there should be no problem concerning mass transport.[3–5] However, since our goal was to create systems that would perform size-selective reactions, we could not use PAFs that might be too large for the reaction to be size-selective.

The reaction condition where alcohol was the solvent also presented another challenge which was the production of unwanted products. In most of our test reactions where acetaldehyde and ethanol were put together, we observed the production of acetaldehyde diethyl acetal especially when the reaction was running at high temperature and even when no PAF was present in the reaction. Similar result was found when ethanol was replaced by methanol which produced acetaldehyde dimethyl acetal instead. Although the formation of acetals was not entirely unexpected, we did not expect that it would become so significant since usually acidic condition is required for acetal formation.[8,9] It would also be against our purpose if we were to use other

solvent instead of ethanol since eventually the reaction setup for ethanol upgrading would have to be done in ethanol.

On the other hand, C3-symmetric receptors were found to have potential as size-selective hydrogen-bond catalysts, although with some significant limitations. Our receptor was shown to have the ability to distinguish between hydrogen-bond acceptors with different shapes such as in the case of n-butylamine and sec-butylamine. It also appeared to catalyze the S_N2 reaction between cinnamyl chloride and aniline to some extent. Nevertheless, it is clear that the reactivity of the receptor is not yet satisfactory since it only works with one case of substrate pair with an unimpressive yield so far while in other cases, either the catalyst did not help improving the yield or the background reaction was too fast that no difference between having and not having the catalyst can be observed.

Concerning reactivity of receptor, we were disappointed that we were unsuccessful in the synthesis of the fluorinated C3-symmetric receptor as described in Chapter 3.2. We believe that electronegative fluorine atoms in the naphthol ring would help increase acidity of the hydroxyl group, which would then increase the strength of hydrogen bond it is capable of forming and potentially improve its catalytic properties.

Another challenge that we faced with this type of receptors was the relatively low solubility, which is the problem also found in at least one other report.[10] As mentioned in Chapter 3.1, our original C3-symmetric receptor was found to be insoluble in common organic solvents at room temperature, which prevented it from further reaction and from being useful as a catalyst. Although we were able to improve the solubility by adding flexible alkyl chain to each naphthol ring, the solubility was still not great in non-polar solvent, which would limit its use in some types

of reactions where specific solvent is needed. This challenge would also be a factor that we have to keep in mind if we were to design new receptors with similar structure.

Although we suspected that the low reactivity might be caused by inhibition from the chloride ions released from the reaction, it is worth noting that reaction yield did not improve in direct proportion when more catalyst was used, even at stoichiometric amount. This led us to consider that the catalyst might not be stable over the course of reaction. Another evidence for the possible decomposition of the catalyst is that the catalyst solution usually changed color over time from light red to dark red (in $CHCl_3$) within few hours. ^1H NMR spectrum of the catalyst solution also showed new peaks in the aromatic region when the solution was left for a significant amount of time. Nevertheless, the catalyst was stable in its solid form when kept at room temperature in N_2 atmosphere for at least a few months.

References

(1) Trewin, A.; Cooper, A. I. *Angew. Chemie - Int. Ed.* **2010**, *49* (0), 1533–1535.
(2) Pei, C.; Ben, T.; Qiu, S. *Mater. Horiz.* **2015**, *2* (1), 11–21.
(3) Verde-Sesto, E.; Merino, E.; Rangel-Rangel, E.; Corma, A.; Iglesias, M.; Sánchez, F. *ACS Sustain. Chem. Eng.* **2016**, *4* (3), 1078–1084.
(4) Rangel-Rangel, E.; Verde-Sesto, E.; Rasero-Almansa, A. M.; Iglesias, M.; Sánchez, F. *Catal. Sci. Technol.* **2016**, *6* (15), 6037–6045.
(5) Merino, E.; Verde-Sesto, E.; Maya, E. M.; Iglesias, M.; Sánchez, F.; Corma, A. *Chem. Mater.* **2013**, *25* (6), 981–988.
(6) Zhang, Y.; Li, B.; Ma, S. *Chem. Commun.* **2014**, 1–6.
(7) Palmer, R. D. Mass Transport in Metal-Organic Frameworks As a Limiting Step in Size-Selective Oligomerization, Massachusetts Institute of Technology, 2016.
(8) Adams, E. W.; Adkins, H. *J. Am. Chem. Soc.* **1925**, *47* (5), 1358–1367.
(9) Adkins, H.; Adams, E. W. *J. Am. Chem. Soc.* **1925**, *47* (5), 1368–1381.
(10) Sather, A. C.; Berryman, O. B.; Moore, C. E.; Rebek, J. *Chem. Commun.* **2013**, *49* (57), 6379–6381.

5.0 Conclusion

Porous aromatic frameworks PAF-1 and PPN-3 were found to be unsuitable platforms for selective-oligomerization despite having impressive properties both in term of surface area and stability. Synthesis and functionalization of PAFs were successful, but functionalized PAFs showed undesired reactivity possibly due to low rate of substrate and product diffusion in and out of the framework. On the other hand, C3-symmetric receptor was found to exhibit some potential for selectivity and catalysis. It was demonstrated that the receptor was able to distinguish substrates with different functional groups in binding experiments, and was able to improve S_N2 reaction yield although with some significant limitations.

6.0 Supporting Information (SI)

6.1 Methods and Instrumentation

All reagents were purchased from commercial sources and used without further purification. NMR spectra were recorded on a Bruker AVANCE 400 MHz spectrometer. TGA measurements were performed on a Mettler Toledo TGA/DSC 2 equipped with a GC 200 gas flow controller, and a Julabo F 25 chiller. Decomposition measurements were performed by subjecting approximately 5 mg of PAFs to the temperature range of 30 °C to 700 °C under 5 mL/min N_2 atmosphere with the temperature ramp rate of 1 °C/min. IR data were recorded on Thermo Scientific Nicolet iS5 FT-IR Spectrometer with iD5 ATR accessory.

The procedure for carbon dioxide absorption measurement of PAFs including the TGA method used was as followed: Approximately 5 mg of PAF was subjected to 50 mL/min N_2 atmosphere at 30 °C for 2 minutes, then heated to 120 °C at the rate of 5 °C/min and held at this temperature for 10 minutes to remove solvent and water residue. The sample was then cooled down to 25 °C at the rate of -50 °C/min and held for 25 minutes to allow complete cooling. After that, the temperature was increased from 25 °C to 30 °C at the rate of 5 °C/min, and the N_2 atmosphere was replaced by CO_2 atmosphere with the same gas flow rate of 50 mL/min. The CO_2 atmosphere was held for 15 minutes and was replaced back to N_2 atmosphere for another 5 minutes. The amount of CO_2 absorption is calculated using the average weight difference of the sample under N_2 and CO_2 atmospheres.

The general procedure for NMR binding studies was as followed: 10.0 mg (9.74×10^{-3} mmol) of the C3-symmetric receptor and 97.4×10^{-3} mmol of guest compound were separately dissolved in 3 mL $CDCl_3$ to make stock solutions. Each set of 12 NMR samples was prepared by adding appropriate amount of the two stock solutions and an additional amount of $CDCl_3$ to bring

the total volume in each NMR tube to 0.7 mL. Exact amount used is shown below in Table S1. Association constants (K_a) were calculated using a Matlab-based analysis program written by Lowe, Pfeffer, and Thordarson, which is publicly available online (*ThordarsonFittingProgram*).[1] All calculation was run on Matlab R2016a by MathWorks, Inc.

Sample	Host Equiv.	Guest Equiv.	Host Stock Solution (μL)	Guest Stock Solution (μL)	Additional $CDCl_3$ (μL)
1	1	0.1	200	2	498
2	1	0.3	200	6	494
3	1	0.5	200	10	490
4	1	0.7	200	14	486
5	1	0.9	200	18	482
6	1	1.2	200	24	476
7	1	1.5	200	30	470
8	1	1.8	200	36	464
9	1	2.7	200	54	446
10	1	3.6	200	72	428
11	1	10.8	200	216	284
12	1	21.6	200	432	68

Table S1. Amount of host and guest used for preparation of the NMR binding studies.

6.2 Synthesis of Materials

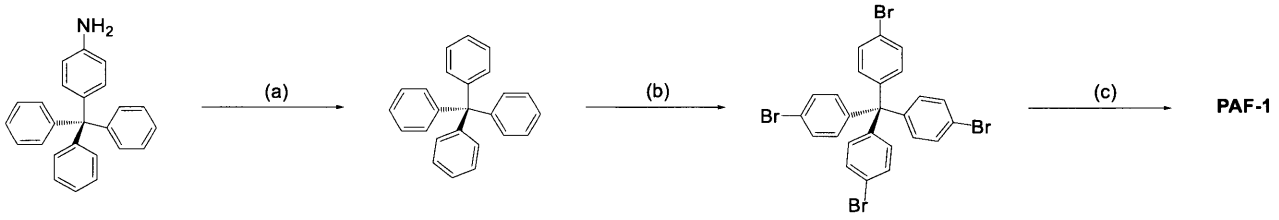

Scheme S1. Schematic for the synthesis of PAF-1

tetraphenylmethane (S1).

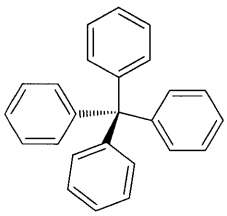

Procedure adapted from literature.[2] 4-tritylaniline (3.02 g, 9.0 mmol) was suspended in DMF (25 mL) and cooled to –15 °C. Sulfuric acid (2.75 mL) and isoamyl nitrite (2.05 mL) were added slowly and the solution was stirred for 1 h. Hypophosphoric acid (50% in water, 4.5 mL) was added dropwise. The reaction mixture was then heated to 50 °C until there was no gas evolution. The solid was filtered off and washed with DMF (25 mL), water (25 mL), and ethanol (25 mL). The washing was repeated twice. The solid was recrystallized in chloroform/methanol mixture and used immediately in the next step.

tetrakis(4-bromophenyl)methane (S2).

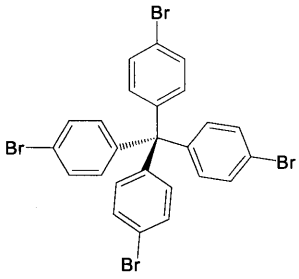

Procedure adapted from literature.[2] To a three-necked round-bottomed flask containing bromine (9.0 mL, 170 mmol, 20 equiv), tetraphenylmethane (S1) (2.4 g, 7.5 mmol, 1 equiv) was slowly added at room temperature. After the addition was completed, the reaction mixture was stirred for 20 min and then cooled to –78 °C. Ethanol (30 mL) was added slowly and the reaction mixture was allowed to warm to room temperature overnight. The solid was filtered off and washed with sodium hydrogensulfite solution (25 mL) and water (25 mL). It was then

recrystallized in chloroform/methanol mixture. After drying in vacuo, the product was obtained as a yellow solid (1.08 g, 19% from two steps).

PAF-1 (S3).

Procedure adapted from literature.[3] 1,5-Cyclooctadiene (1.17 mL, 9.51 mmol, 5.6 equiv) was added to the solution of bis(1,5-cyclooctadiene)nickel(0) (2.60 g, 9.51 mmol, 5.6 equiv) and 2,2′-bipyridyl (1.48 g, 9.51 mmol, 5.6 equiv) in dehydrated DMF (130 mL). The reaction mixture was then heated to 80 °C and stirred for 1 h. To the resulting dark purple solution, tetrakis(4-bromophenyl)methane (S2) (1.08 g, 1.69 mmol, 1 equiv) was added, and the reaction mixture was stirred at that temperature for 72 h. After cooling to 0 °C, concentrated HCl (50 mL) was added to the reaction mixture, and the reaction mixture was stirred at room temperature for another 48 h. The solid was filtered off then washed with chloroform (5 x 30 mL), THF (5 x 30 mL), water (5 x 30 mL), and was purified by Soxhlet extraction with THF for 24 h, then chloroform for 24 h. The resulting solid was filtered off and dry in vacuo to give PAF-1 as an off-white powder. (345 mg, 65%)

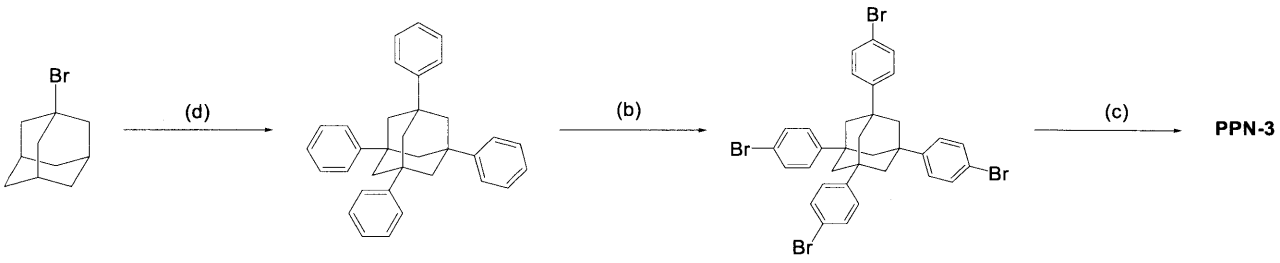

Scheme S2. Schematic for the synthesis of PPN-3

1,3,5,7-tetraphenyladamantane (S4).

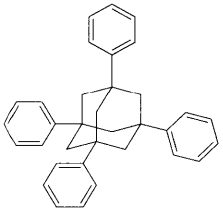

Procedure adapted from literature.[2] 1-Bromoadamantane (3.0 g, 13.9 mmol, 1 equiv) was dissolved in benzene (30 mL) under N_2 atmosphere at room temperature. *t*-Butyl iodide (3.5 mL, 27.8 mmol, 2 equiv) and aluminum

chloride (0.16 g, 1.39 mmol, 0.1 equiv) were added to the solution. The solution mixture was then refluxed overnight. The reaction mixture was cooled to room temperature and the precipitate was filtered off and washed with chloroform (25 mL), water (25 mL), and chloroform (25 mL). The product was dried in vacuo overnight and was obtained as a slightly red solid (possible contaminated color from the rubber septum) and was used immediately in the next step.

1,3,5,7-tetrakis(4-bromophenyl)adamantine (TBPA) (S5).

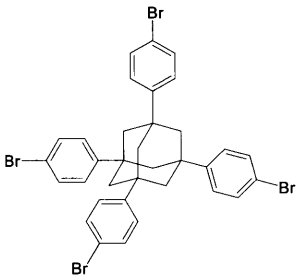

Procedure adapted from literature.[2] To a three-necked round-bottomed flask containing tetraphenyladamanthane (3.0 g, 6.8 mmol, 1 equiv), bromine (3.5 mL, 68 mmol, 10 equiv) was slowly added at room temperature. After the addition was completed, the reaction mixture was stirred for 20 min and then cooled to –78 °C. Ethanol (30 mL) was added slowly and the reaction mixture was allowed to warm to room temperature overnight. The solid was filtered off and washed with sodium hydrogensulfite solution (25 mL) and water (25 mL). The solid was put in methanol (25 mL) and stirred for 1 h at 40 °C. It was then filtered off and recrystallized in chloroform/methanol mixture. After drying in vacuo, the product was obtained as a white solid (2.26 g. 20% from two steps).

PPN-3 (S6).

Procedure adapted from literature.[3] 1,5-Cyclooctadiene (1.17 mL, 9.51 mmol, 5.6 equiv) was added to the solution of bis(1,5-cyclooctadiene)nickel(0) (2.60 g, 9.51 mmol, 5.6 equiv) and 2,2′-bipyridyl (1.48 g, 9.51 mmol, 5.6 equiv) in dehydrated DMF (130 mL). The reaction mixture was then heated to 80 °C and stirred for 1 h. To the resulting dark purple solution, 1,3,5,7-tetrakis(4-bromophenyl)adamantine (S5) (1.25 g, 1.65 mmol, 1 equiv) was added, and the reaction mixture was stirred at that temperature for 72 h. After cooling to 0 °C, concentrated HCl (50 mL) was added

to the reaction mixture, and the reaction mixture was stirred at room temperature for another 48 h. The solid was filtered off then washed with chloroform (5 x 30 mL), THF (5 x 30 mL), water (5 x 30 mL), and was purified by Soxhlet extraction with THF for 24 h, then chloroform for 24 h. The resulting solid was filtered off and dry in vacuo to give PPN-3 as a white powder (0.48 g, 67%).

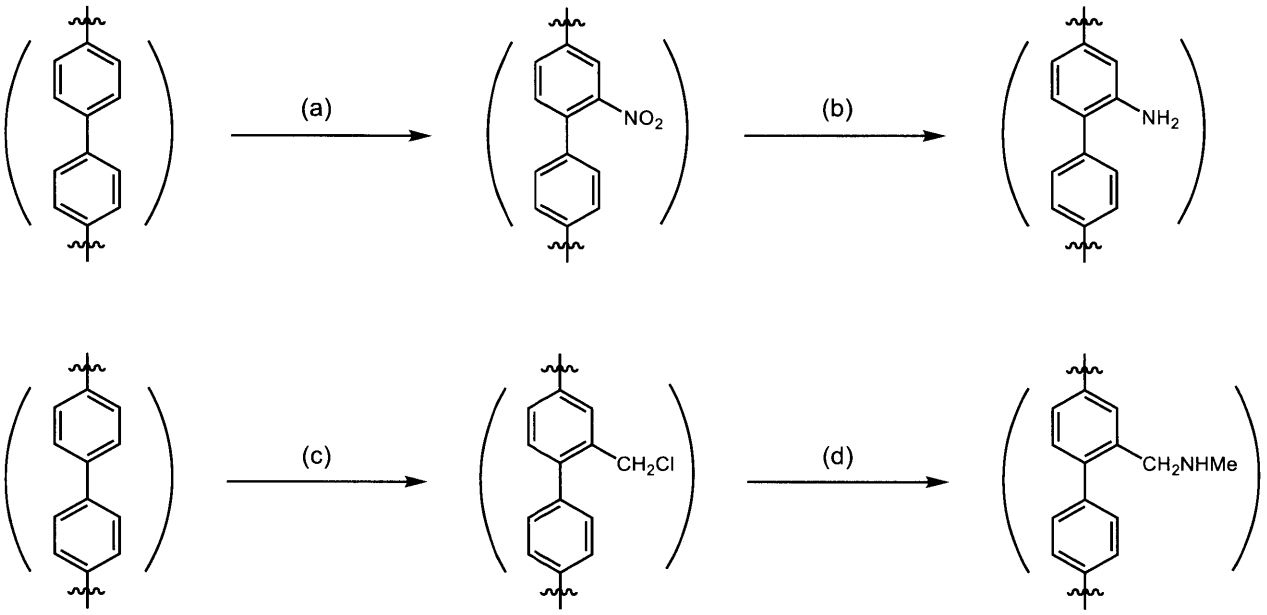

Scheme S3. Schematic for the synthesis of functionalized PAF-1 and PPN-3.

PAF-1-NH_2 (S7a) and PPN-3-NH_2 (S7b).

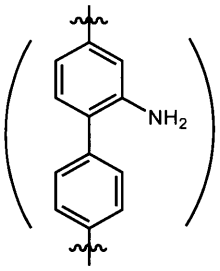

Procedure followed directly from literature.[4] PAF-1 (100 mg) or PPN-3 (140 mg) was put in N_2 atmosphere in an oven-dried 40 mL vial. Acetic anhydride (7 mL) and CH_2Cl_2 (7 mL) were added to the vial, and the reaction mixture was cooled to 0 °C. Copper (II) nitrate hemi(pentahydrate) (1.61 g, 6.92 mmol) was added portionwise over five minutes. The reaction mixture was allowed to warm to room temperature, and stirred for 24 h. Solid PAF-1-NO_2 or PPN-3-NO_2 was filtered off, washed with HCl (3 N, 2 x 20 mL), hot water (3 x 20 mL), hot ethanol (5 x 20 mL), and left to air dry over vacuum for 15 min. The solid was then immediately suspended in 1:1 methanol:water (12 mL

each) under N_2. Sodium dithionite (1.4 g, 8.0 mmol) was added, and the reaction was heated to 70 °C and stirred for 24 h. The solid was filtered off, and suspended in hot water (30 mL) for 1 h. The hot water was replaced by pure hot water by syringe, and the cycle was repeated five times, followed by two cycles of 60 °C ethanol. After filtration, the solid was washed with hot THF (5 x 20 mL) to give the desired material as a white powder, which was activated under vacuum at 80 °C for 16 hours to provide the product PAF-1-NH_2 (76 mg, 72%) or PPN-3-NH_2 (67 mg, 65%).

PAF-1-CH_2Cl (S8a) and PPN-3-CH_2Cl (S8b).

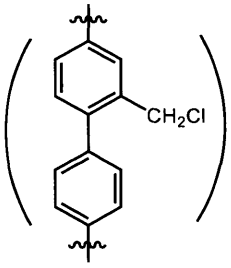

Procedure followed directly from literature.[5] PAF-1 (200 mg) or PPN-3 (280 mg), paraformaldehyde (1.0 g), glacial AcOH (6.0 mL), H_3PO_4 (3.0 mL), and concentrated HCl (20 mL) were added to a reaction flask. The flask was sealed and heated to 90 °C for 3 days. The solid was filtered off, washed with water and methanol, resulting in a brown powder PAF-1-CH_2Cl (370 mg, 160% (wet)) or PPN-3-CH_2Cl (340 mg, 155% (wet)).

PAF-1-CH_2NHMe (S9a) and PPN-3-CH_2NHMe (S9b).

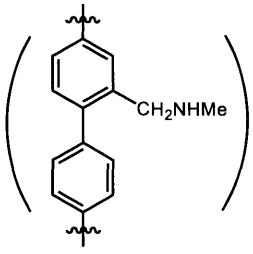

Procedure adapted from literature.[5] PAF-1-CH_2Cl or PPN-3-CH_2Cl (50 mg) and methylamine (40% in water, 3 mL) were added to a vial. The reaction vial was sealed and heated to 80 °C for 3 days. The resulting solid was filtered off, washed with water and methanol, and then dried in vacuo to produce PAF-1-CH_2NHMe (36 mg, 61%) or PPN-3-CH_2NHMe (77 mg, 113%) respectively as a brown powder.

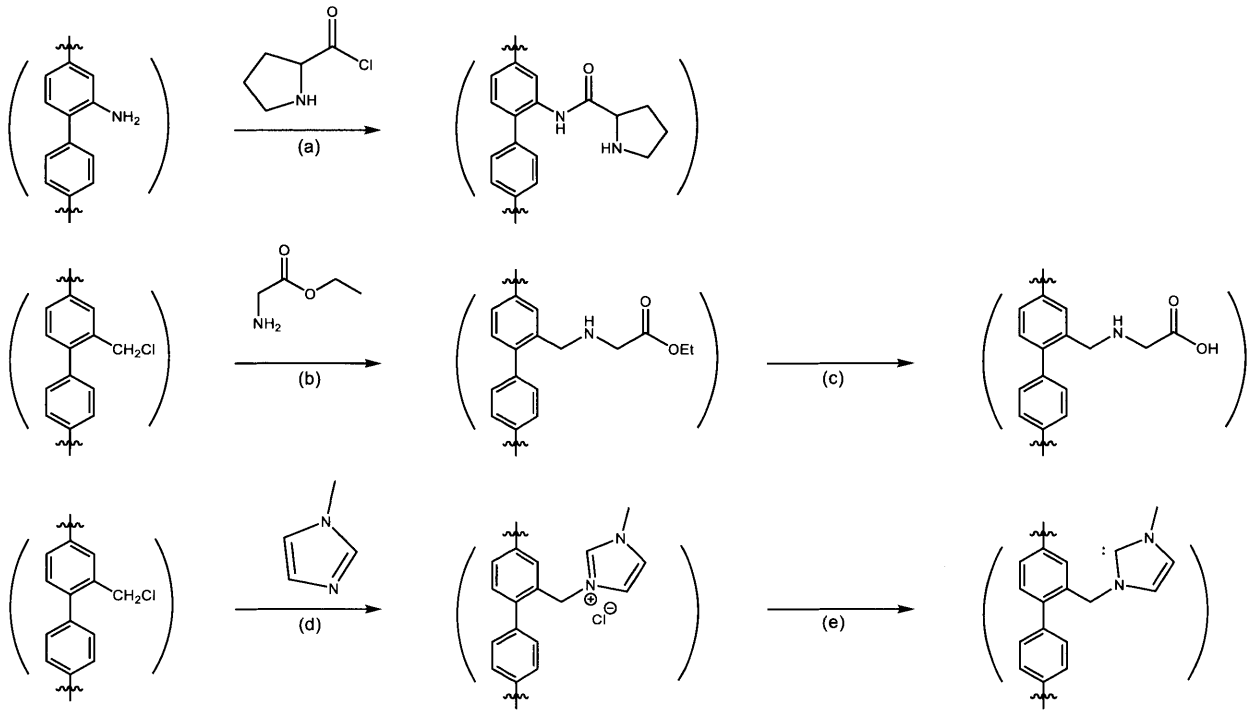

Scheme S4. Schematic for the synthesis of the second set of functionalized PAF-1.

PAF-1-Proline (S10).

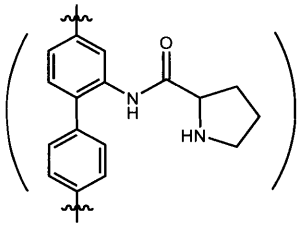

PAF-1-NH_2 (30 mg, 1 equiv), proline acid chloride (120 mg, 10 equiv), and THF (2 mL) were added to a 20 mL vial. The reaction mixture was then stirred at room temperature for 24 h. The resulting solid was filtered off, washed with water and methanol, and then dried in vacuo resulting in a dark brown solid. (25.2 mg, 64%)

PAF-1-Glycine (S11).

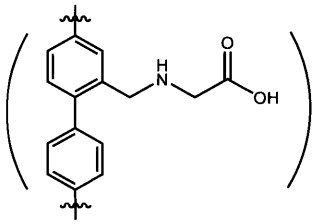

PAF-1-CH_2Cl (50 mg, 1 equiv), glycine ethyl ester (350 mg, 20 equiv), triethylamine (0.4 mL, 20 equiv), and toluene (10 mL) were added to a 40 mL vial. The reaction mixture was heated to 80 °C and stirred overnight. Water (25 mL) was added, and the reaction mixture was

stirred for another 1 h. The resulting solid was filtered off, washed with water and methanol, and then dried in vacuo resulting in a dark brown solid (19 mg, 33%).

PAF-1-NHC (S12).

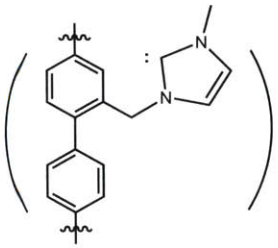

1-methylimidazole (0.44 mL, 20 equiv) was added to the suspension of PAF-1-CH_2Cl (100 mg, 1 equiv) in toluene (3 mL) at 0 °C. The reaction mixture was then allowed to warm to room temperature and then heated to 65 °C for 24 h. The resulting solid was filtered off, washed with toluene, and then dried in vacuo to give PAF-1-imidazole-Cl. PAF-1-imidazole-Cl (40 mg, 1 equiv) was then subsequently put into another vial. *t*-BuOK (13 mg, 1.3 equiv) was added, followed by THF (2 mL). The reaction mixture was stirred at room temperature for 48 h. The resulting solid was filtered off, washed with THF, water, methanol, and then dried in vacuo at 120 °C for 24 h to give a yellow solid (28 mg, 25%).

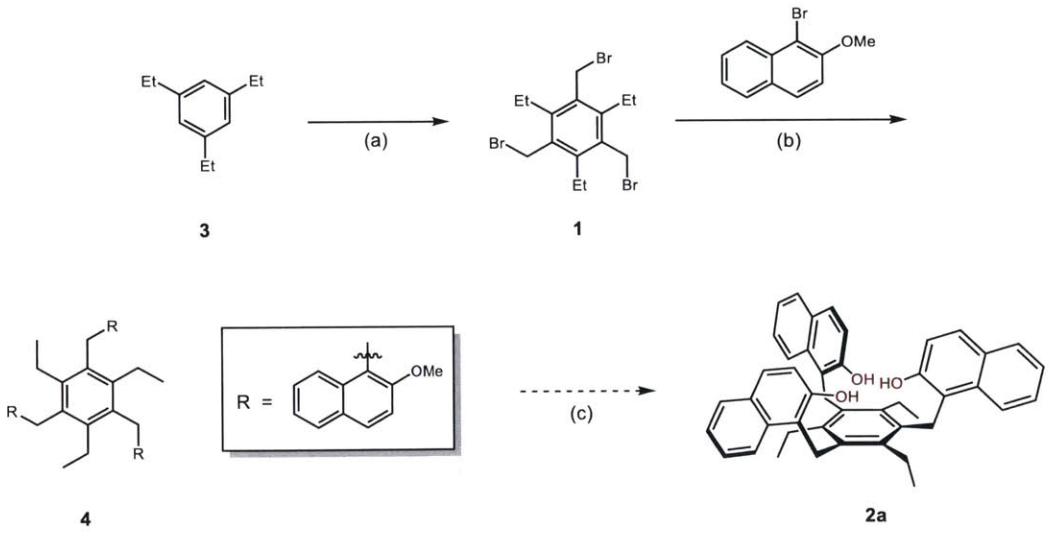

Scheme S5. Schematic for the synthesis of the original C3-symmetric receptor catalyst.

1,3,5-tris(bromomethyl)-2,4,6-triethylbenzene (1).

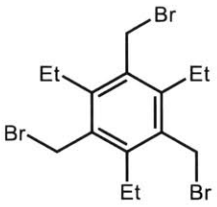

Procedure adapted from literature.[6] Triethylbenzene (1.0 mL, 1 equiv) and paraformaldehyde (1.67 g, 10 equiv) were dissolved in hydrobromic acid solution 33 wt. % in acetic acid (10 mL). Zinc bromide (1.97 g, 1.6 equiv) was added to the reaction mixture slowly at room temperature. The solution was heated to 90 °C for 16.5 h. After cooling to room temperature, the white precipitate was filtered and washed with water (3 x 10 mL), then dried in vacuo for 10 h (2.59 g, >95%). ^{1}H NMR (δ, $CDCl_3$): 4.58 (s, 6H), 2.94 (q, J = 7.6 Hz, 6H), 1.34 (t, J = 7.6 Hz, 9H).

methoxy-protected original C3-symmnetric receptor catalyst (4).

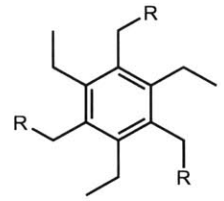

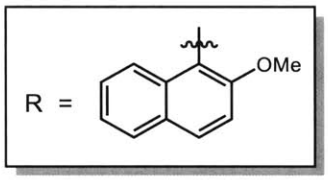

Magnesium turning (220 mg, 9.04 mmol, 6 equiv) and 2-3 crystals of iodine was added to a flame-dried 40 mL vial under N_2 atmosphere. The vial was heated with a heat gun to activate the magnesium. The solution of 1-bromo-2-methoxynaphthalene (1.78 g, 7.53 mmol, 5 equiv) in anhydrous THF (20 mL) was transferred slowly into the vial with magnesium at room temperature. The reaction mixture was heated to 55 °C and stirred for 2 h until the solution turned dark grey or black, indicating the formation of the Grignard reagent. The reaction mixture was then transferred to a reaction flask containing 1,3,5-tris(bromomethyl)-2,4,6-triethylbenzene (1) (664 mg, 1.51 mmol, 1 equiv) and copper (I) iodide (287 mg,1.51 mmol, 1 equiv) in THF (10 mL) at room temperature. The reaction mixture was heated to 55 °C and stirred overnight. After cooling to room temperature, water (100 mL) was added, and the resulting solid was filtered off and washed with water to give the product as a white solid (830 mg ,82%). ^{1}H NMR (δ, $CDCl_3$): 7.78 (s, 3H), 7.69 (m, 6H), 7.24 – 7.15 (m, 6H), 6.83 (br.s, 3H), 4.51 (s, 6H), 3.60 (br.s, 9H), 2.78 (q, J = 7.4 Hz, 6H), 0.92 (t, J = 7.4 Hz, 9H).

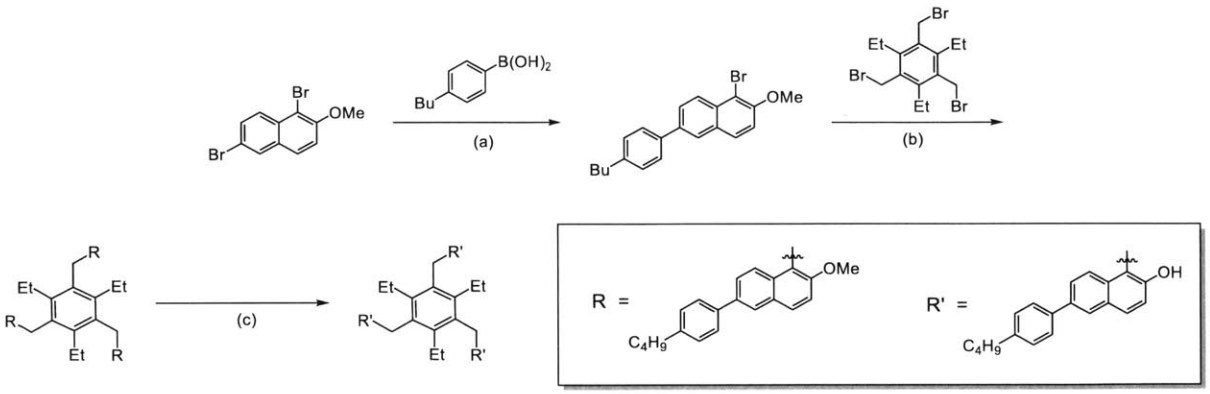

Scheme S6. Schematic for the synthesis of the modified C3-symmetric receptor catalyst.

1-bromo-6-(4-butylphenyl)-2-methoxynaphthalene (S13).

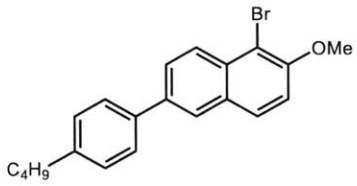

1,6-Bromo-2-methoxynaphthalene (1.5 g, 4.75 mmol, 1 equiv), 4-butylphenyl boronic acid (846 mg, 4.75 mmol, 1 equiv), K_2CO_3 (1.32 g, 9.5 mmol, 2 equiv), and $Pd(PPh_3)_4$ (63 mg, 0.0475 mmol, 0.01 equiv) were added to a reaction flask under N_2 atmosphere. Toluene/water/methanol (30 mL/15 mL/15 mL) was then added, and the reaction mixture was heated to 80 °C and stirred for 18 h. HCl (3 N, 25 mL) was added, and the reaction mixture was extracted with DCM, then washed with water and brine. The organic extract was dried over Na_2SO_4, concentrated, and recrystallized in methanol to give white crystals (1.1 g, 63%). ^{1}H NMR (δ, $CDCl_3$): 8.27 (d, J = 8.9 Hz, 1H), 7.97 (d, J = 1.8 Hz, 1H), 7.90 – 7.79 (m, 2H), 7.67 – 7.59 (m, 2H), 7.30 (dd, J = 8.6, 1.9 Hz, 3H), 4.05 (s, 3H), 2.72 – 2.64 (m, 2H), 1.72 – 1.60 (m, 2H), 1.41 (h, J = 7.4 Hz, 2H), 0.96 (t, J = 7.3 Hz, 3H). HRMS (DART) calculated for $C_{21}H_{21}BrO$ (M^+) 368.0770, found 368.0768.

methoxy-protected modified C3-symmetric receptor catalyst (S14).

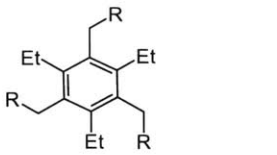

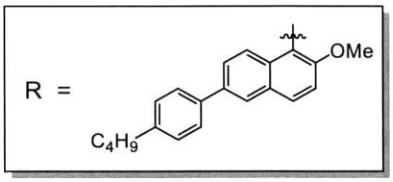

Magnesium turning (200 mg, 8.1 mmol, 6 equiv) and 2-3 crystals of iodine was added to a flame-dried 40 mL vial under N_2 atmosphere. The vial was heated with a heat gun to activate the magnesium. The solution of 1-bromo-6-(4-butylphenyl)-2-methoxynaphthalene (S13) (2 g, 5.42 mmol, 4 equiv) in anhydrous THF (20 mL) was transferred slowly into the vial with magnesium at room temperature. The reaction mixture was heated to 55 °C and stirred for 2 h until the solution turned dark grey or black, indicating the formation of the Grignard reagent. The reaction mixture was then transferred to a reaction flask containing 1,3,5-tris(bromomethyl)-2,4,6-triethylbenzene (1) (597 mg, 1.35 mmol, 1 equiv) and copper (I) iodide (257 mg,1.35 mmol, 1 equiv) in THF (10 mL) at room temperature. The reaction mixture was heated to 55 °C and stirred overnight. After cooling to room temperature, water (100 mL) was added, and the resulting solid was filtered off and washed with water to give the product as a light gray solid (1.14 g,79%). ^{1}H NMR (δ, $CDCl_3$): 7.98 – 7.87 (m, 3H), 7.83 – 7.67 (m, 6H), 7.62 (d, J = 8.2 Hz, 3H), 7.56 (d, J = 9.6 Hz, 3H), 7.32 – 7.13 (m, 12H), 4.62 – 4.51 (m, 6H), 3.94 (s, 9H), 2.89 – 2.56 (m, 6H), 2.72 – 2.63 (m, 6H), 1.68 – 1.56 (m, 6H), 1.43 – 1.40 (m, 6H), 1.14 – 0.97 (m, 9H), 0.95 (t, J = 7.4, 1.7 Hz, 9H). HRMS (+ESI) calculated for $C_{78}H_{84}O_3$ (M+H) 1069.6493, found 1041.5515.

modified C3-symmetric receptor catalyst (2d).

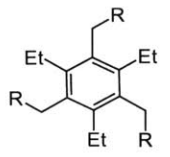

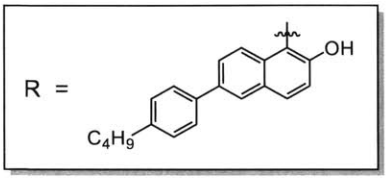

To a suspension of methoxy-protected modified C3-symmetric receptor catalyst (S14) (2.3 g, 2.15 mmol, 1 equiv) in dichloromethane (40 mL) was added BBr_3 (1 M in dichloromethane, 10.8 mL, 10.8 mmol, 5 equiv) slowly at 0 °C. The reaction mixture was allowed to warm to room temperature and stirred for 2 h. The reaction was then quenched with iced water (25 mL), extracted with ethyl acetate, then washed with water and brine. The organic extract was dried over Na_2SO_4, concentrated, then dried under vacuo to give an off-white solid (0.85 g, 39%). ^{1}H NMR (δ, $CDCl_3$): 8.29 (d, J = 8.9 Hz, 3H), 7.98 (d, J = 2.0 Hz, 3H), 7.78 – 7.69 (m, 6H), 7.61 (d, J = 8.1 Hz, 6H), 7.28 – 7.25 (m, 6H), 7.09 (d, J = 8.8 Hz, 3H), 6.08 (s, 3H), 5.30 (s, 6H), 2.82 – 2.54 (m, 6H), 2.72 – 2.64 (m, 6H), 1.64 (q, J = 7.6 Hz, 6H), 1.47 – 1.33 (m, 6H), 1.33 – 1.19 (m, 9H), 0.95 (t, J = 7.3 Hz, 9H). HRMS (+ESI) calculated for $C_{75}H_{78}O_3$ (M+H) 1027.6024, found 1028.8161.

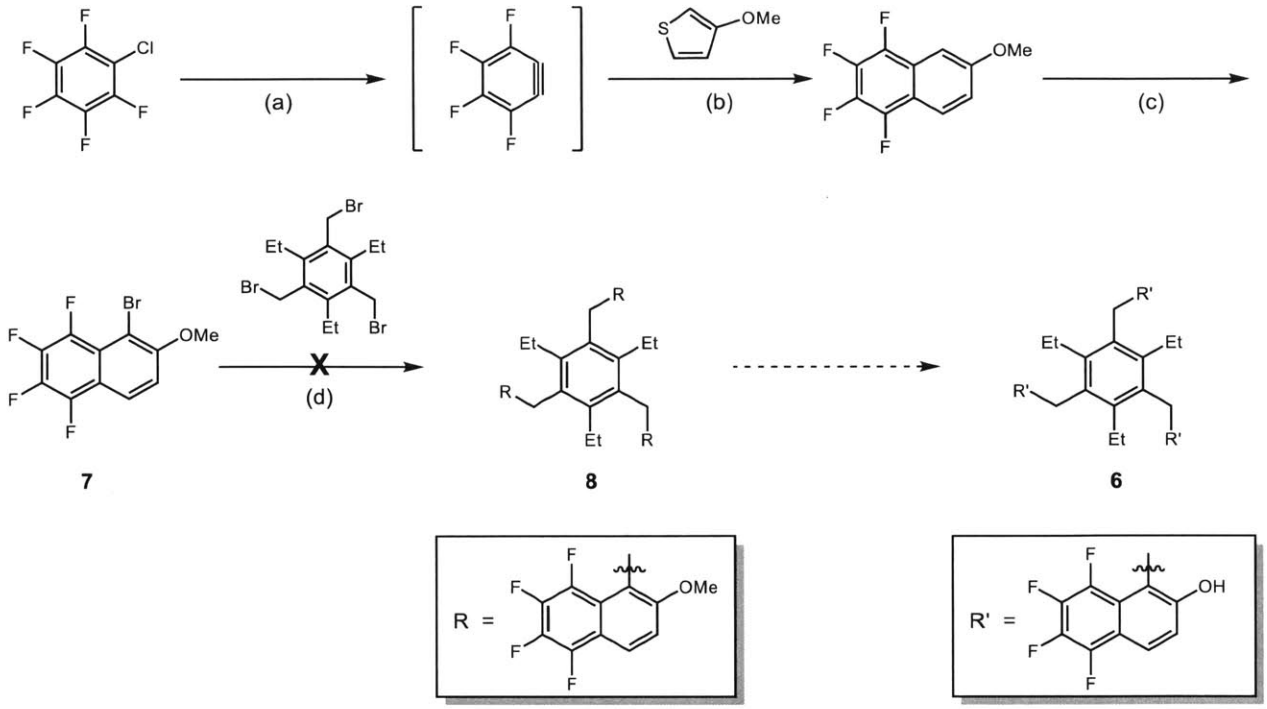

Scheme S7. Schematic for the attempted synthesis of fluorinated C3-receptor catalyst.

2-methoxy-5,6,7,8-tetrafluoronaphthlene (S15).

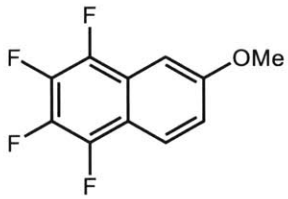

Procedure adapted from literature.[7] To a solution of 3-methoxythiophene (0.99 mL, 10 mmol, 1 equiv) and chloropentafluorobenzene (3.23 mL, 25 mmol, 2.5 equiv) in anhydrous hexane (50 mL) was added *n*-butyllithium (1.6 M solution in hexanes, 12.5 mL, 20 mmol, 2 equiv) dropwise at –15 °C to –20 °C under N_2 atmosphere. The reaction mixture was allowed to warm to room temperature and stirred for 12 h. The reaction mixture was diluted with ether and washed with 5% HCl (25 mL), 5% NaOH (25 mL), and brine (50 mL). The resulting organic extract was dried over Na_2SO_4, concentrated, and chromatographed (hexane:ether, 9:1), and recrystallize in hexane to give white crystals (0.75 g, 33%). ^{1}H NMR (δ, $CDCl_3$): 8.00 – 7.90 (m, 1H), 7.31 – 7.14 (m, 2H), 3.95 (d, J = 1.6 Hz, 3H).

1-bromo-2-methoxy-5,6,7,8-tetrafluoronaphthlene (7).

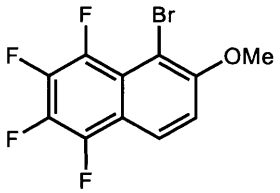

Procedure adapted from literature.[7] To a solution of 2-methoxy-5,6,7,8-tetrafluoronaphthlene (S15) (0.75 g, 3.25 mmol, 1 equiv) in acetonitrile (10 mL) was added *N*-bromosuccinimide (0.72 g, 4.06 mmol, 1.25 equiv). After one hour, the reaction mixture was concentrated, diluted with water and extracted with ether. The resulting organic extract was dried over Na_2SO_4, concentrated, and recrystallized (ethanol:ether, 8:2) to give pale yellow crystals (0.39 g, 39%). ^{1}H NMR (δ, $CDCl_3$): 8.09 – 8.01 (m, 1H), 7.34 (d, J = 9.3 Hz, 1H), 4.05 (d, J = 0.7 Hz, 3H).

References

(1) Lowe, A. J.; Pfeffer, F. M.; Thordarson, P. *Supramol. Chem.* **2012**, *24* (8), 585–594.

(2) Lu, W.; Yuan, D.; Zhao, D.; Schilling, C. I.; Plietzsch, O.; Muller, T.; Bräse, S.; Guenther, J.; Blümel, J.; Krishna, R.; Li, Z.; Zhou, H.-C. *Chem. Mater.* **2010**, *22* (21), 5964–5972.

(3) Ben, T.; Ren, H.; Ma, S.; Cao, D.; Lan, J.; Jing, X.; Wang, W.; Xu, J.; Deng, F.; Simmons, J. M.; Qiu, S.; Zhu, G. *Angew. Chemie - Int. Ed.* **2009**, *48* (50), 9621–9624.

(4) Van Humbeck, J. F.; McDonald, T. M.; Jing, X.; Wiers, B. M.; Zhu, G.; Long, J. R. *J. Am. Chem. Soc.* **2014**, *136* (6), 2432–2440.

(5) Lu, W.; Sculley, J. P.; Yuan, D.; Krishna, R.; Wei, Z.; Zhou, H.-C. *Angew. Chemie - Int. Ed.* **2012**, *124* (30), 7480–7484.

(6) Walsdorff, Christian; Saak, Wolfgang; Pohl, S. *J. Chem. Res. Synopses* **1996**, No. 6, 282–283.

(7) Yudin, A. K.; Martyn, L. J. P.; Pandiaraju, S.; Zheng, J.; Lough, A. *Org. Lett.* **2000**, *2* (1), 41–44.

6.3 Supporting Figures

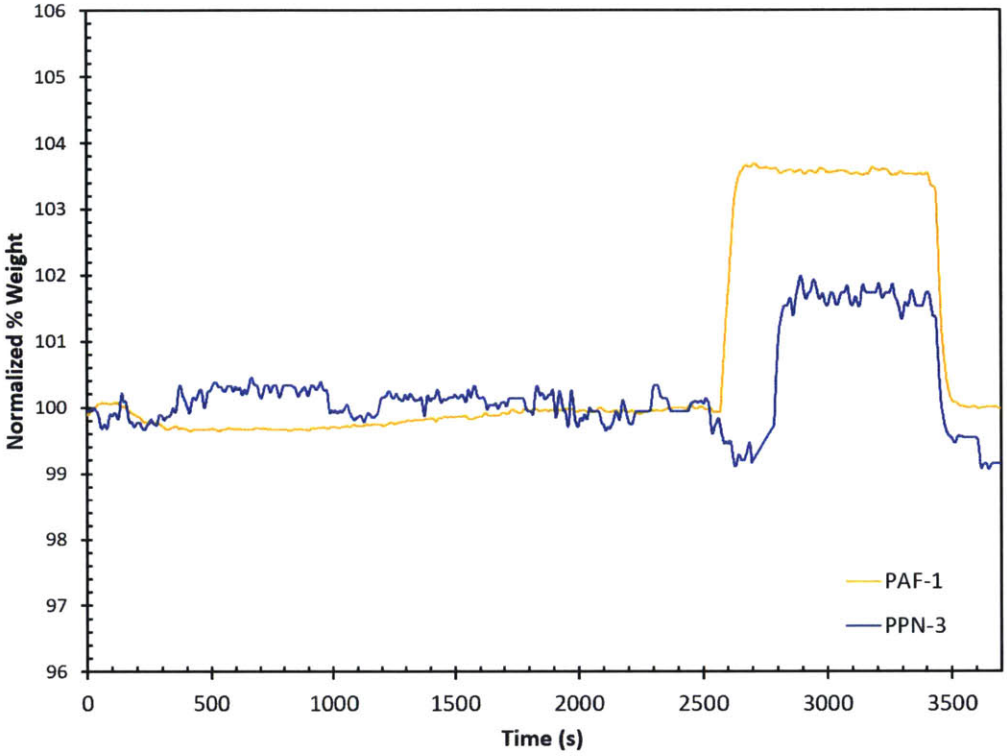

1a

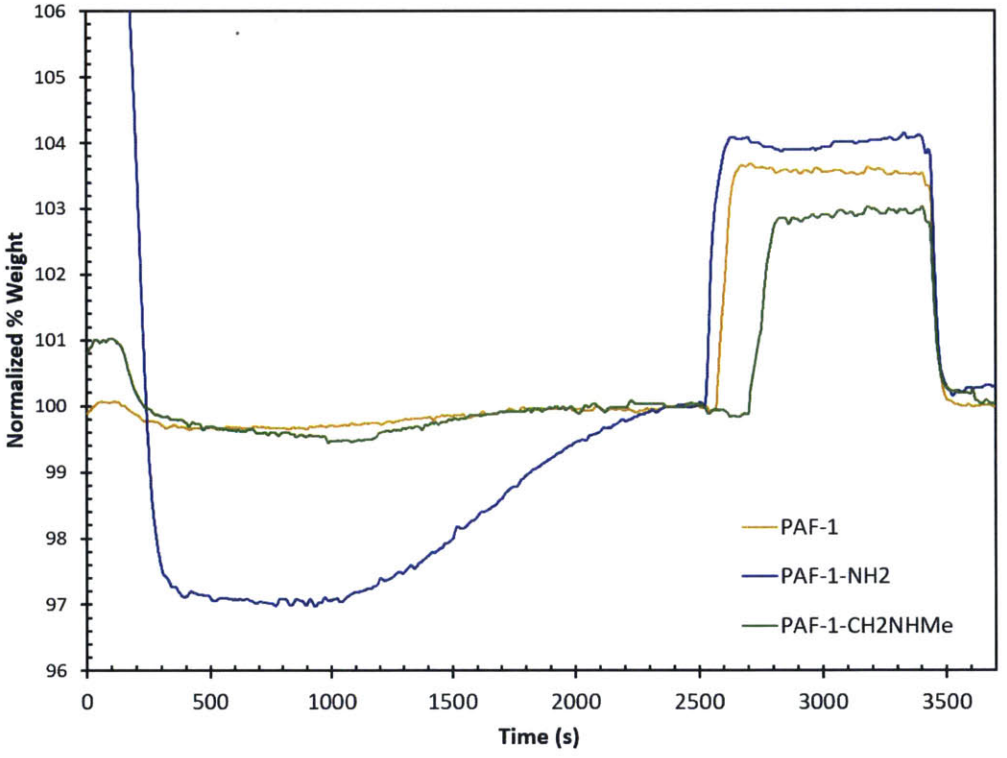

1b

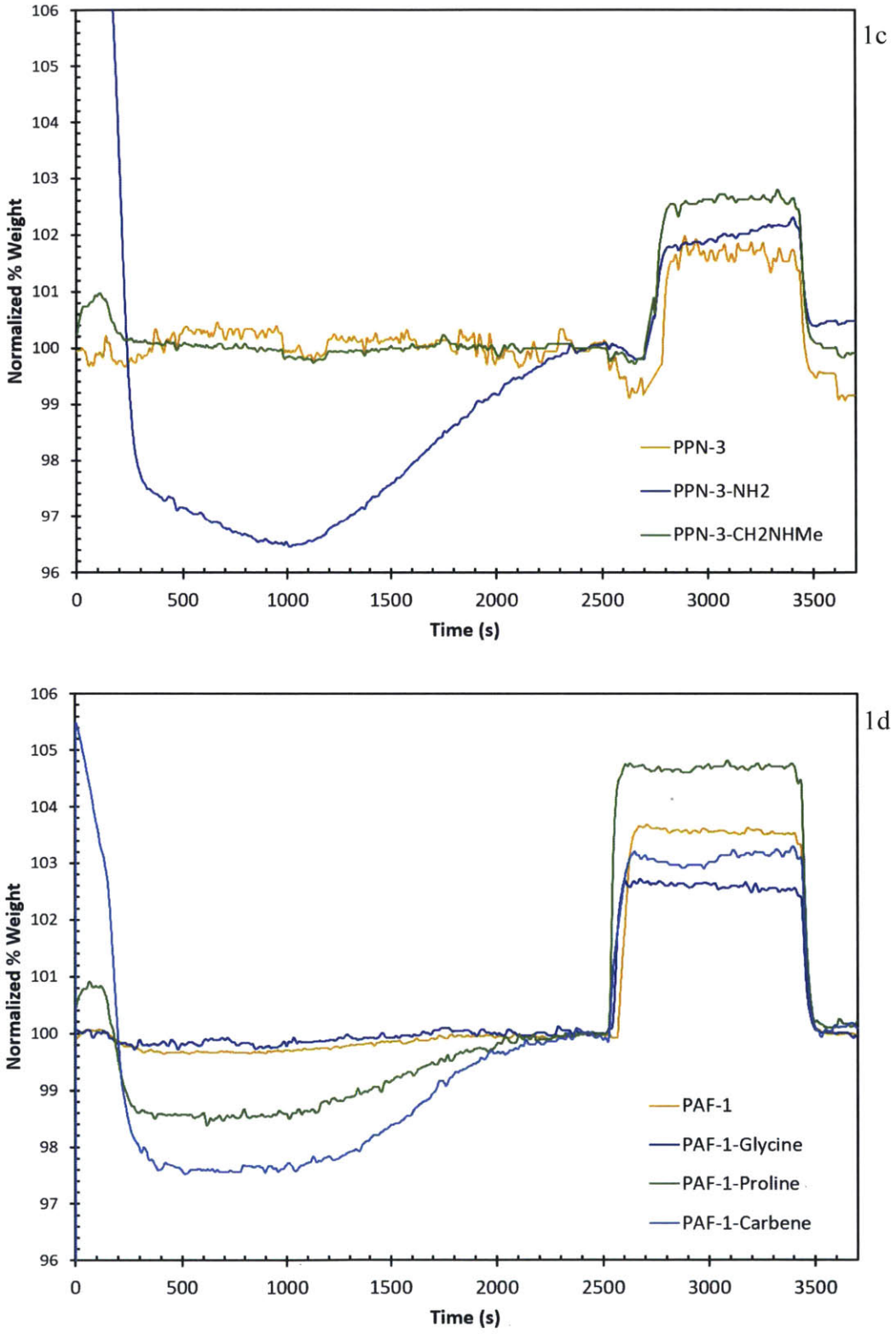

Figure S1. Thermogravimetric data of PAFs for CO_2 absorption. a) PAF-1, PPN-3; b) PAF-1, PAF-1-NH_2, PAF-1-CH_2NHMe; c) PPN-3, PPN-3-NH_2, PPN-3-CH_2NHMe; d) PAF-1, PAF-1-Glycine, PAF-1-Proline, PAF-1-Carbene.

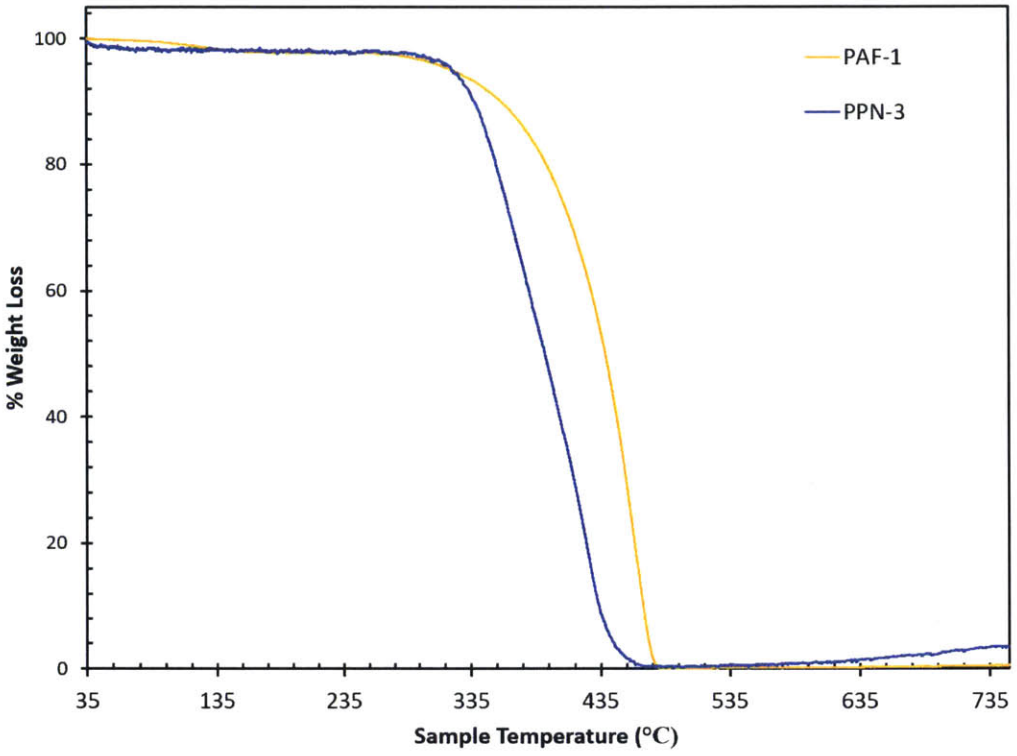
100
80
60
40
20
0
% Weight Loss
35
135
235
335
435
535
635
735
Sample Temperature (°C)
PAF-1
PPN-3

2a

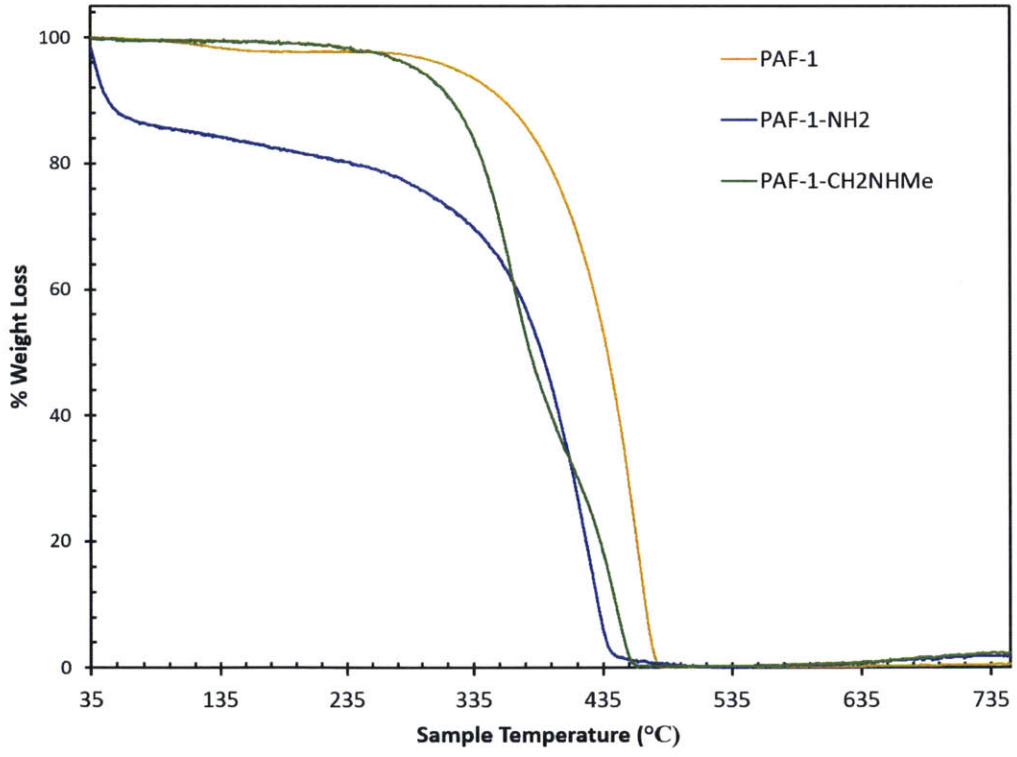
100
80
60
40
20
0
% Weight Loss
35
135
235
335
435
535
635
735
Sample Temperature (°C)
PAF-1
PAF-1-NH2
PAF-1-CH2NHMe

2b

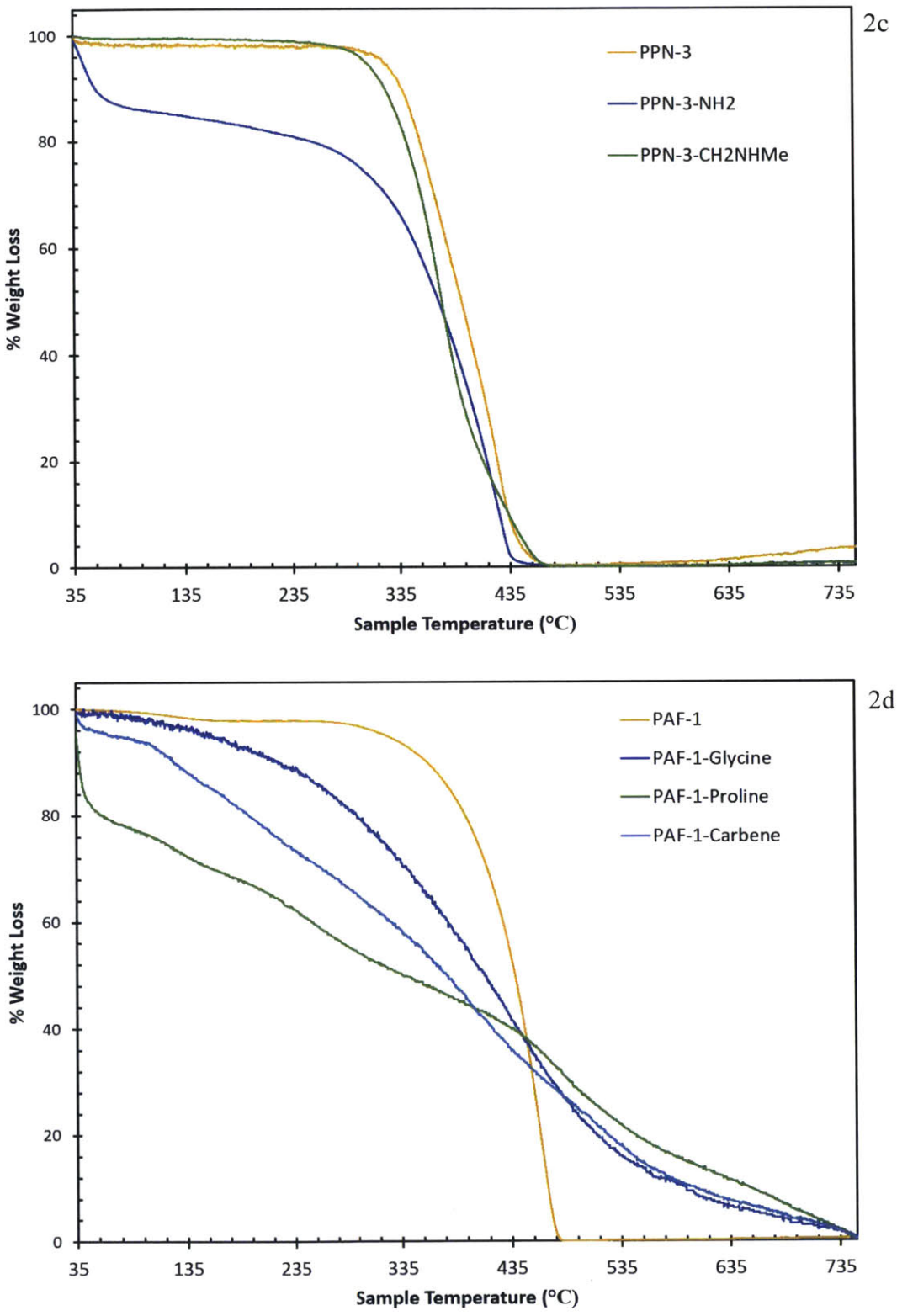

Figure S2. Thermogravimetric data of PAFs for thermal decomposition. a) PAF-1, PPN-3; b) PAF-1, PAF-1-NH_2, PAF-1-CH_2NHMe; c) PPN-3, PPN-3-NH_2, PPN-3-CH_2NHMe; d) PAF-1, PAF-1-Glycine, PAF-1-Proline, PAF-1-Carbene.

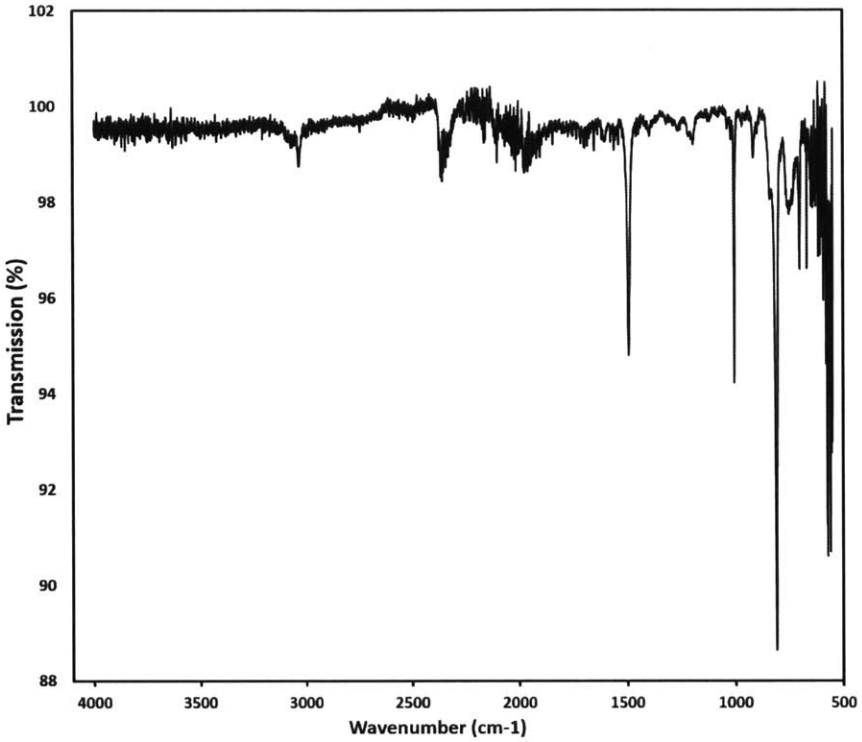

Figure S3. IR spectrum of PAF-1.

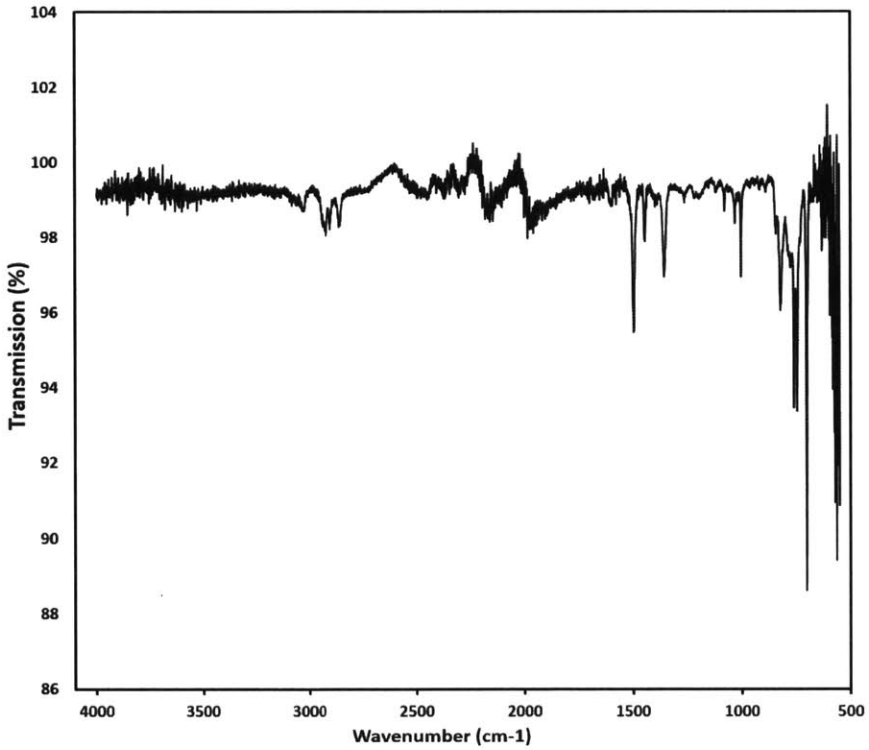

Figure S4. IR spectrum of PPN-3.

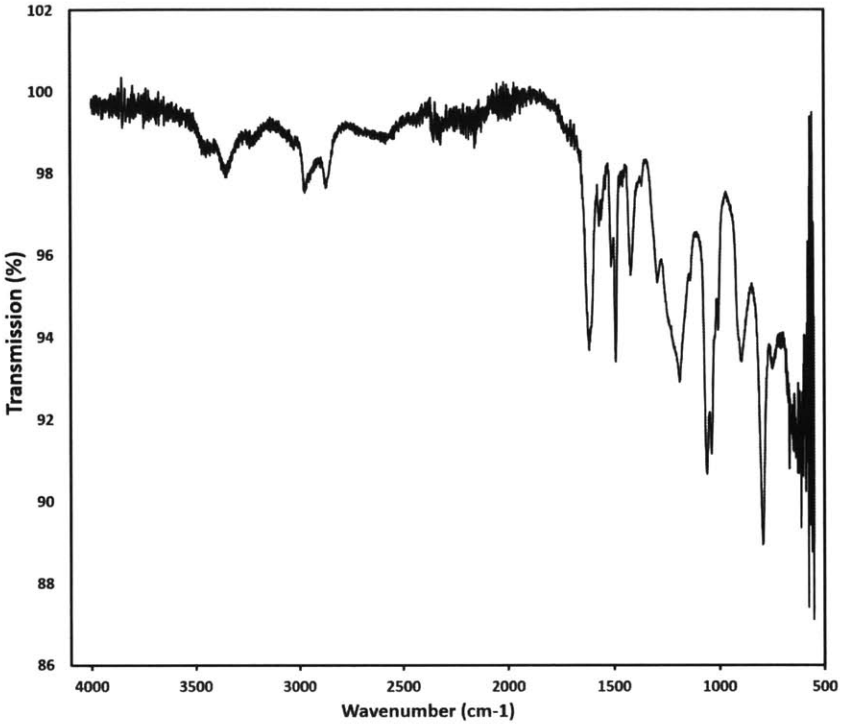

Figure S5. IR spectrum of PAF-1-NH_2.

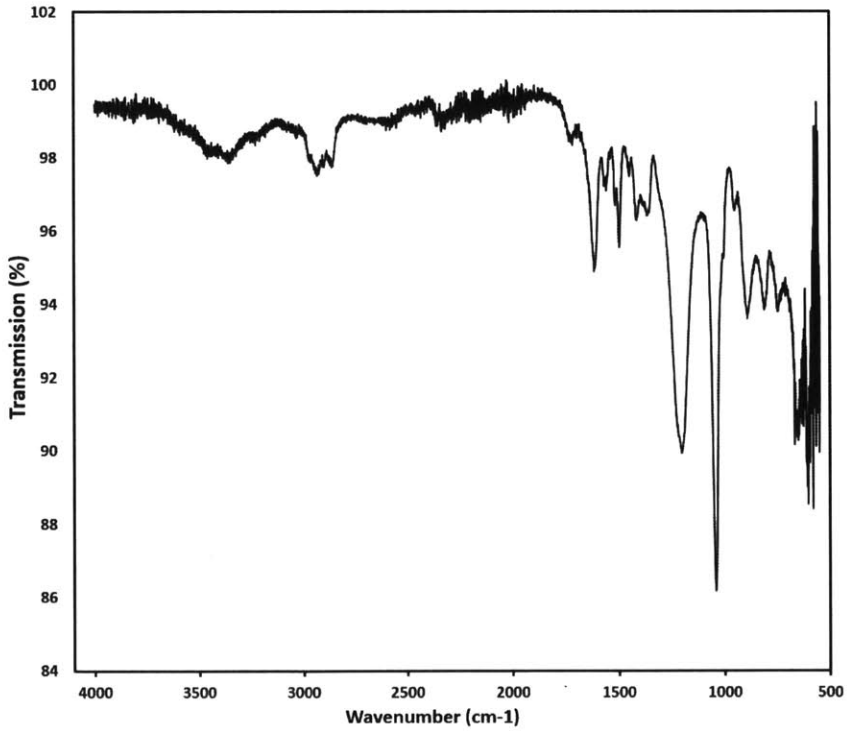

Figure S6. IR spectrum of PPN-3-NH_2.

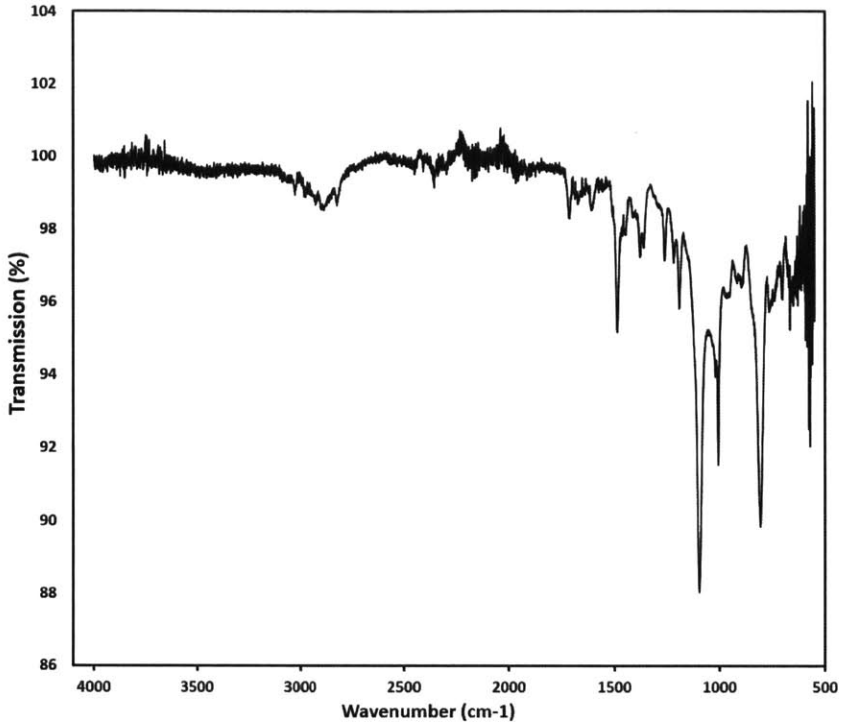

Figure S7. IR spectrum of PAF-1-CH_2NHMe.

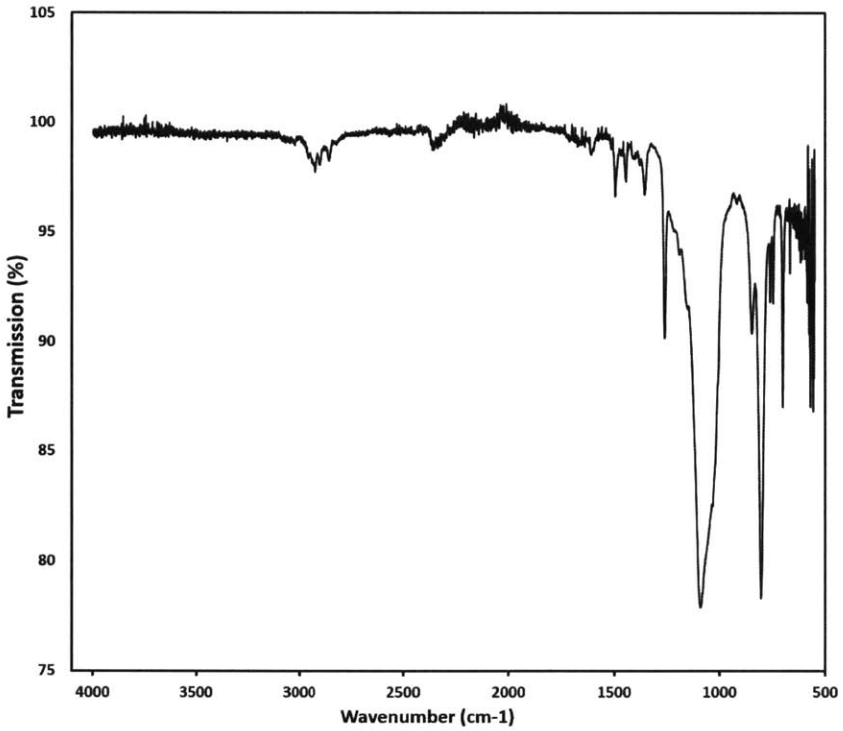

Figure S8. IR spectrum of PPN-3-CH_2NHMe.

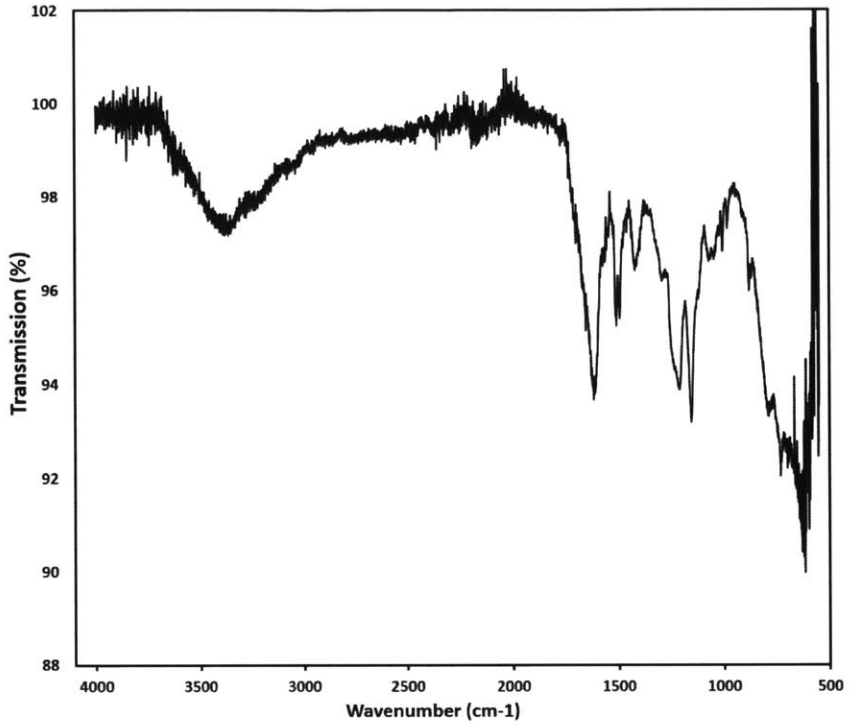

Figure S9. IR spectrum of PAF-1-Proline.

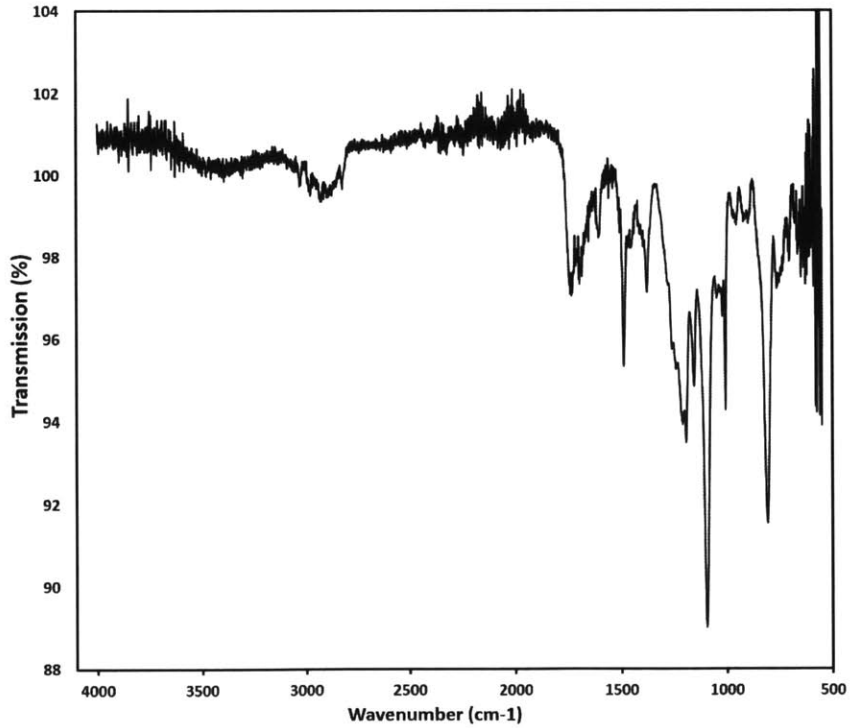

Figure S10. IR spectrum of PAF-1-Glycine.

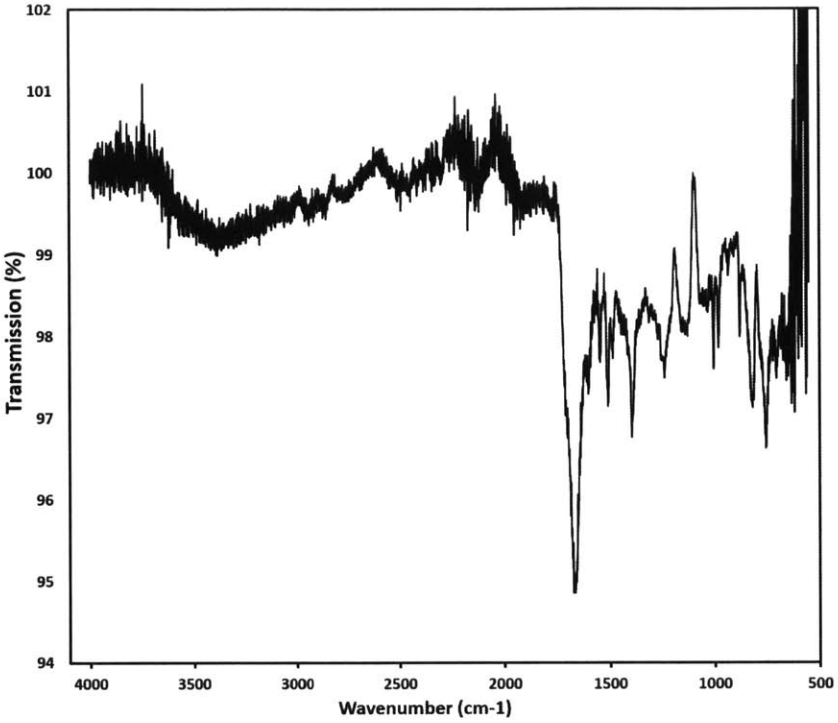

Figure S11. IR spectrum of PAF-1-NHC.

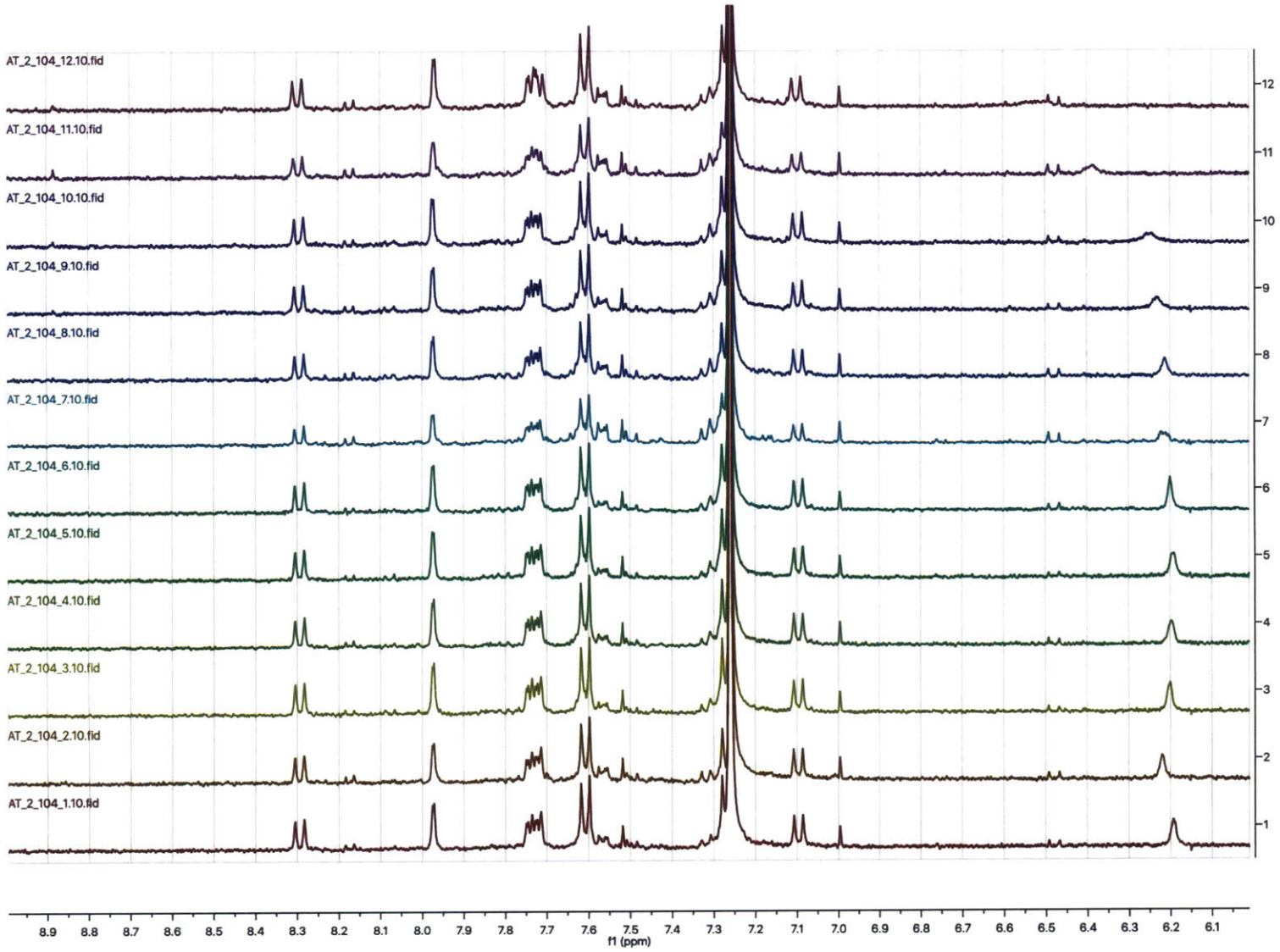

Figure S12. ^{1}H NMR data showing the binding experiment between n-butanol and C3-symmetric receptor. The equivalent between n-butanol and the receptor is increasing from bottom to top from 0.1:1 to 21.6:1. The $CHCl_3$ residual peak is shown at 7.26 ppm.

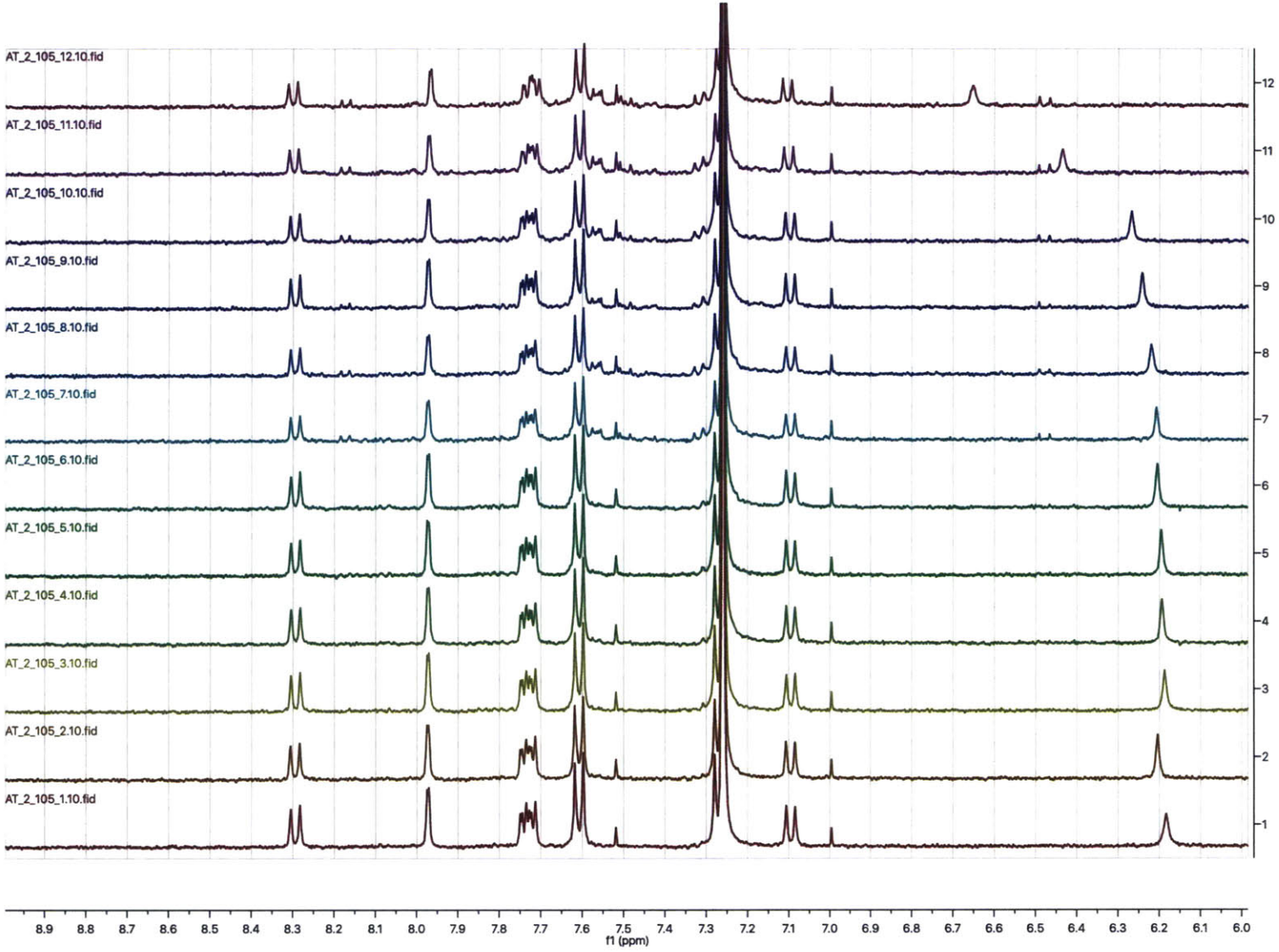

Figure S13. ^{1}H NMR data showing the binding experiment between sec-butanol and C3-symmetric receptor. The equivalent between sec-butanol and the receptor is increasing from bottom to top from 0.1:1 to 21.6:1. The $CHCl_3$ residual peak is shown at 7.26 ppm.

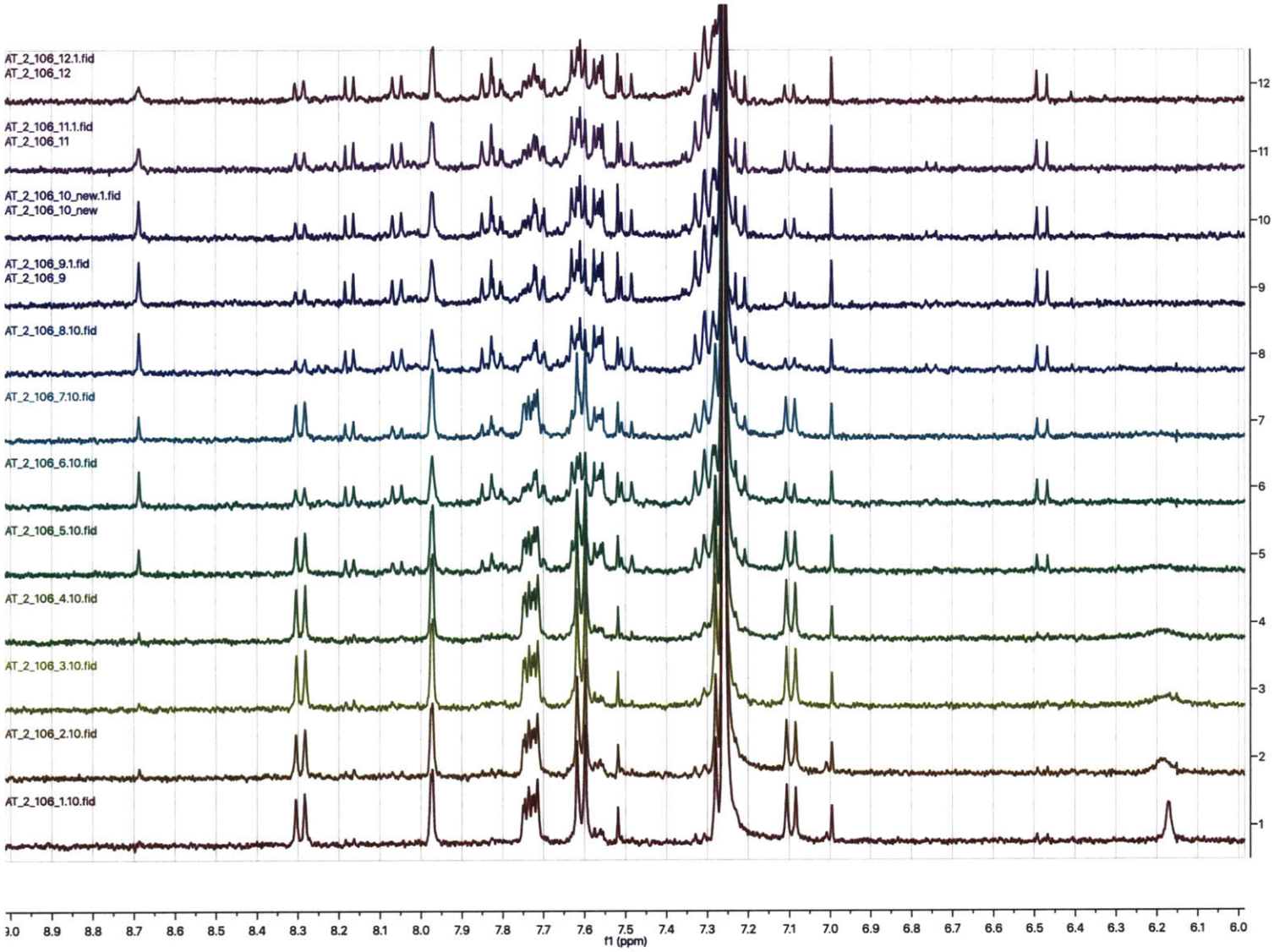

Figure S14. ^{1}H NMR data showing the binding experiment between n-butyric acid and C3-symmetric receptor. The equivalent between n-butyric acid and the receptor is increasing from bottom to top from 0.1:1 to 21.6:1. The $CHCl_3$ residual peak is shown at 7.26 ppm.

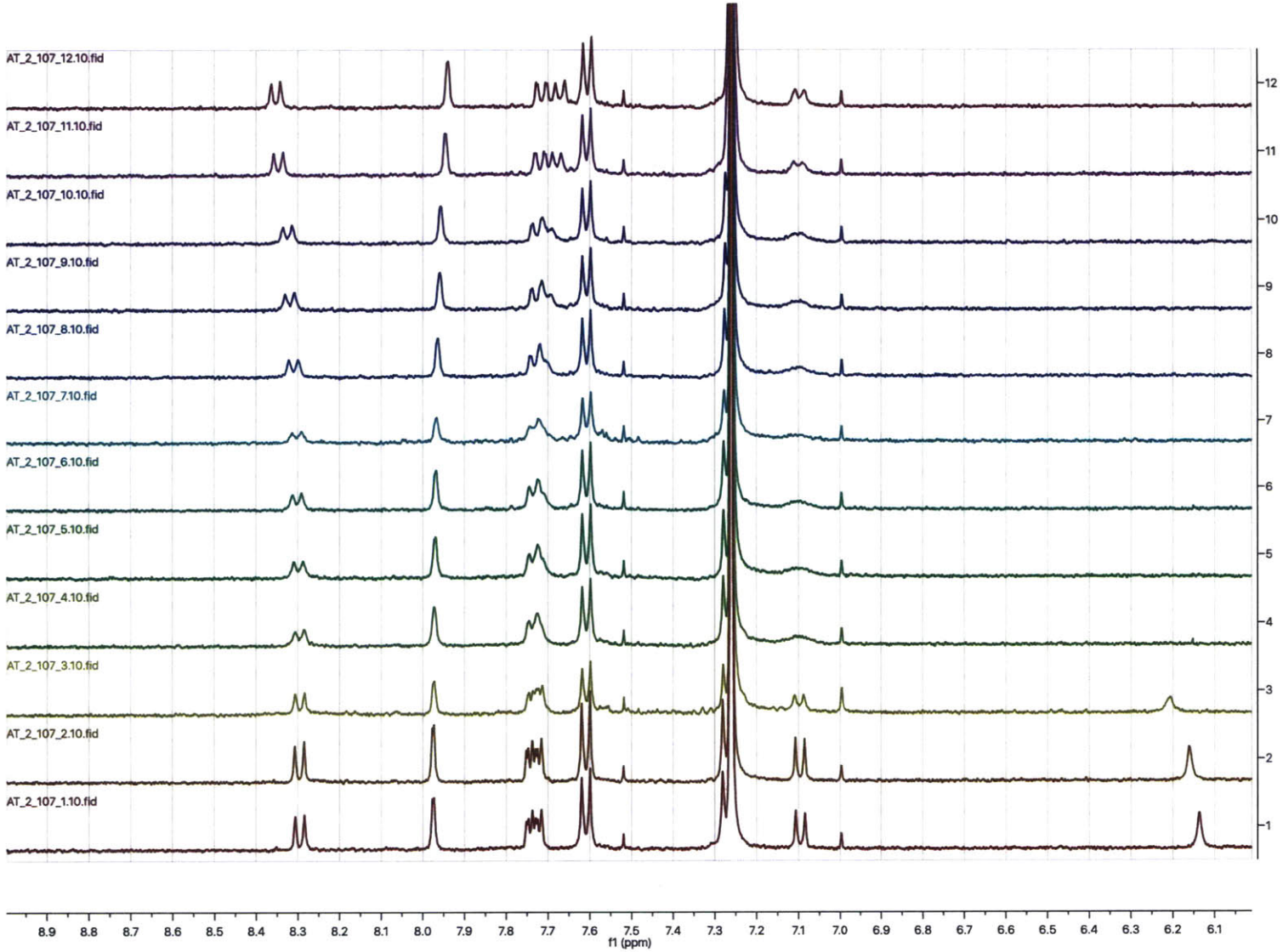

Figure S15. ^{1}H NMR data showing the binding experiment between n-butylamine and C3-symmetric receptor. The equivalent between n-butylamine and the receptor is increasing from bottom to top from 0.1:1 to 21.6:1. The $CHCl_3$ residual peak is shown at 7.26 ppm.

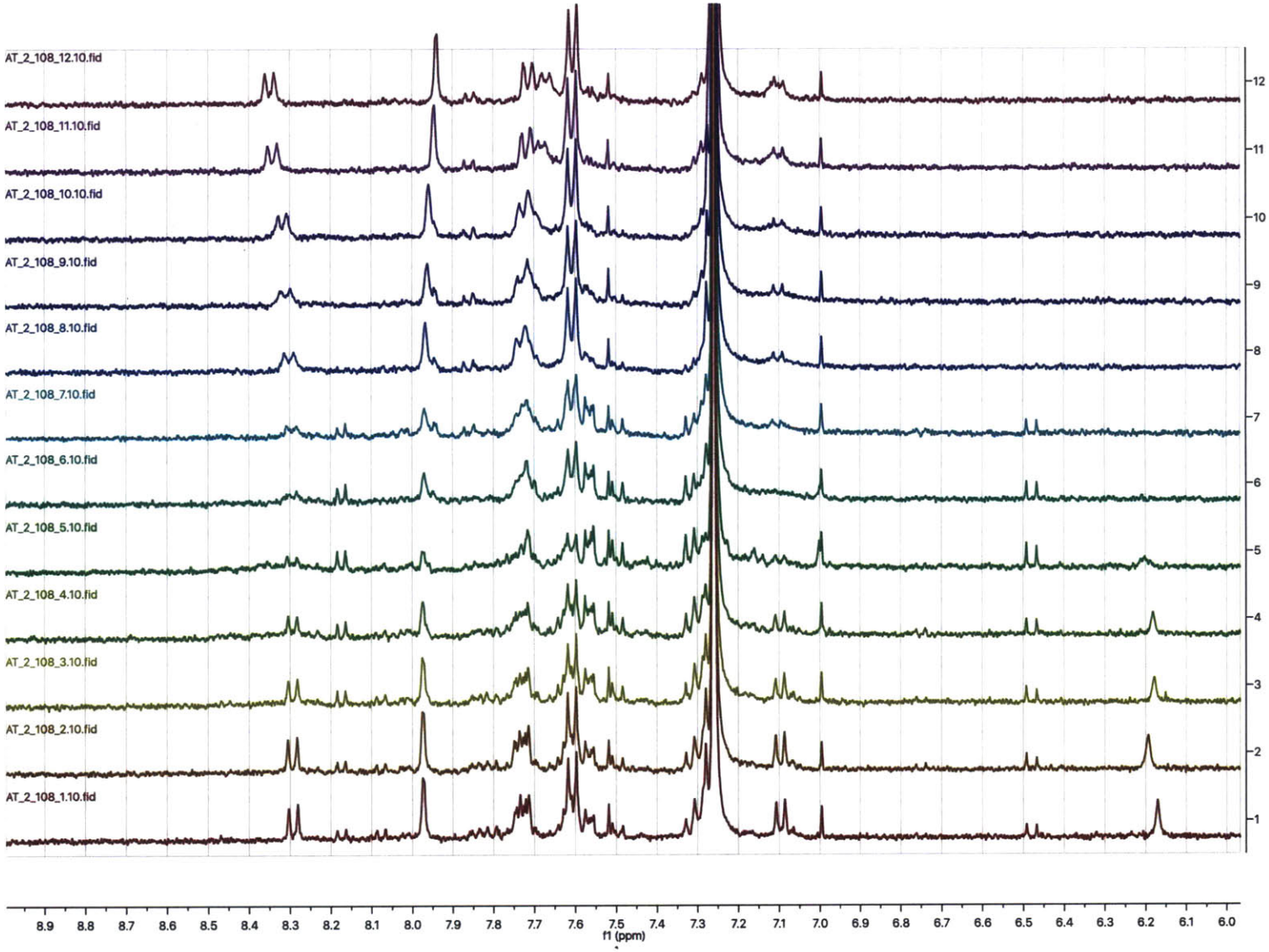

Figure S16. ^{1}H NMR data showing the binding experiment between sec-butylamine and C3-symmetric receptor. The equivalent between sec-butylamine and the receptor is increasing from bottom to top from 0.1:1 to 21.6:1. The $CHCl_3$ residual peak is shown at 7.26 ppm.